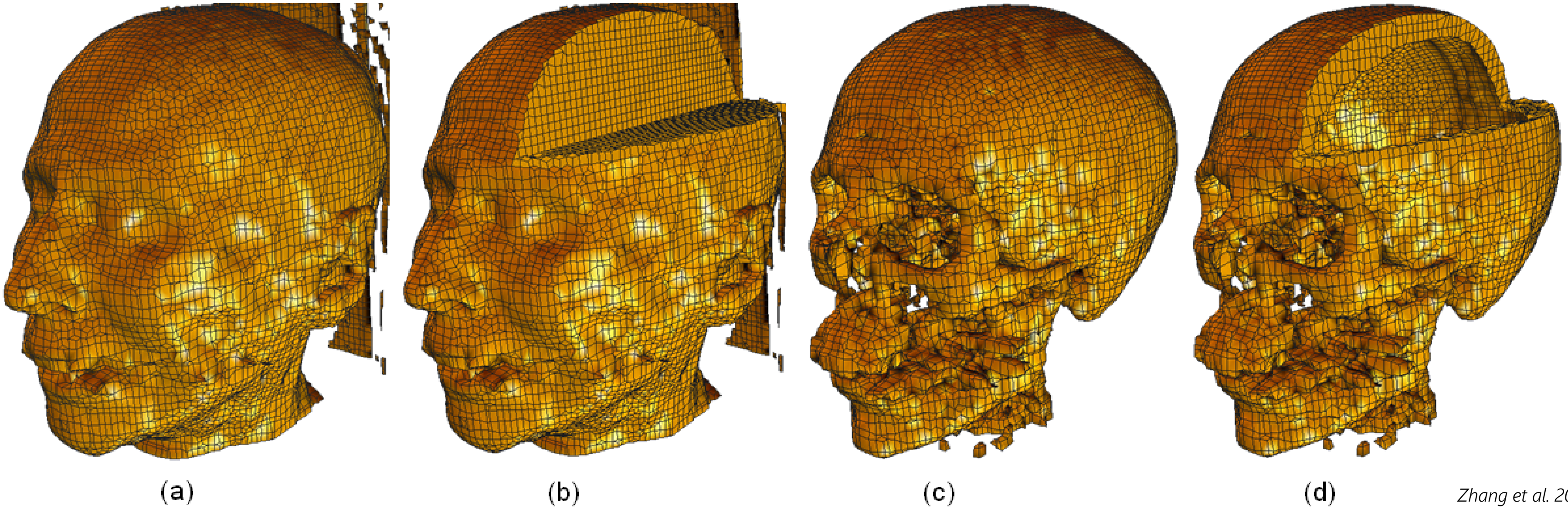

Zhang et al. 2004

Geometry From Imaging Data

Part I: Imaging Techniques
Computational Biomechanics

Summer Term 2016

Lecture 4/12

Frank Niemeyer

Simulation Workflow (FEA, CFD, ...)

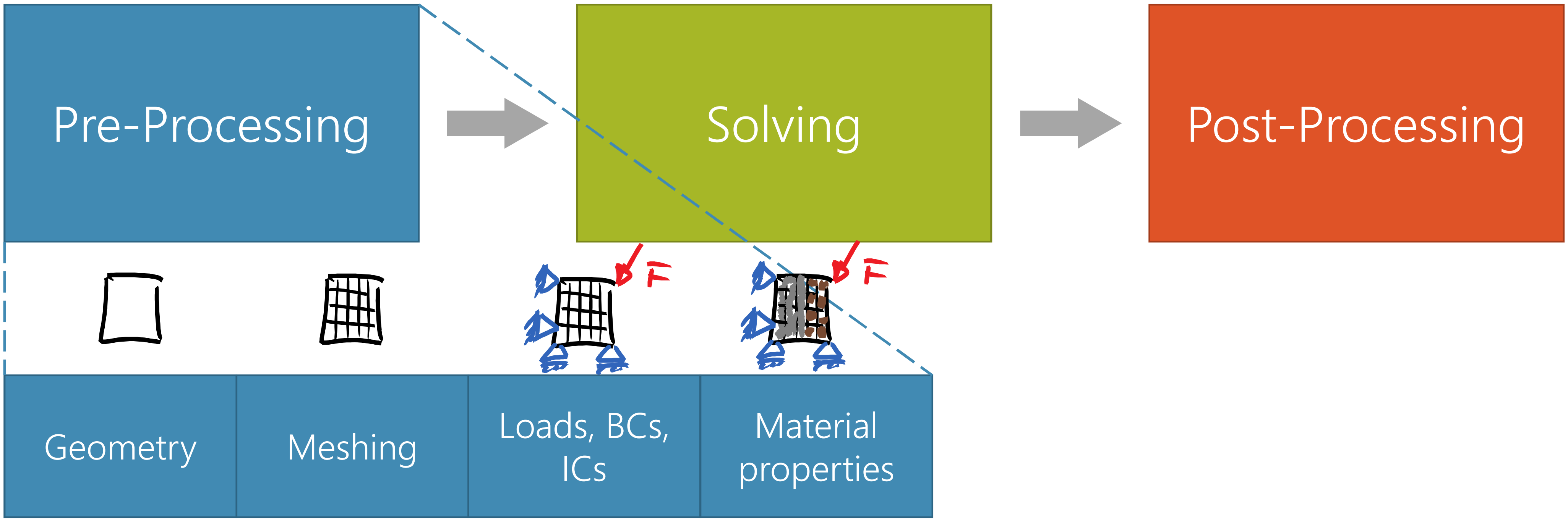

Introduction

Types of Geometry

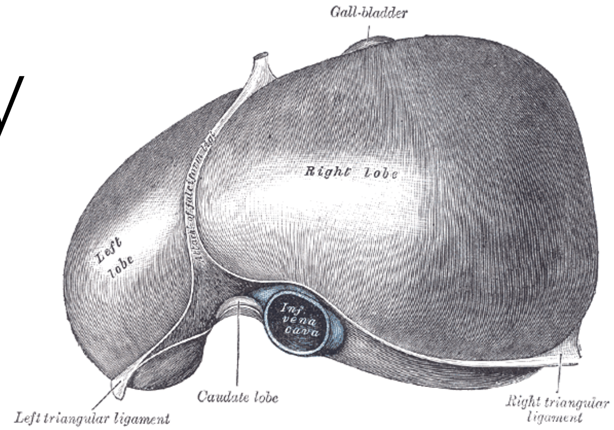

Gray H., Anatomy of the Human Body, 1918

Individual organs

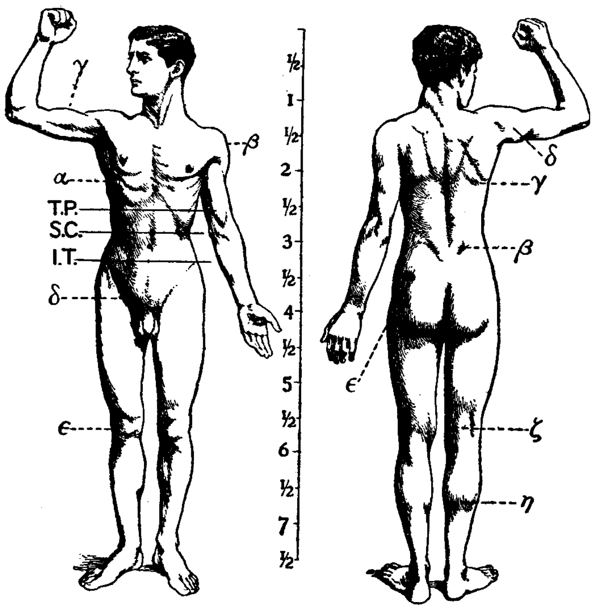

Encyclopædia Britannica Eleventh Edition, vol. 1, p. 940

Outer body shape

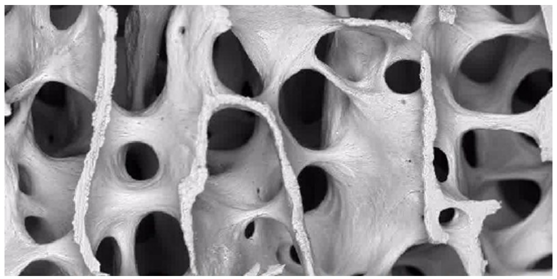

boneresearchsociety.org

Micro-structure

radiopaedia.org

(Blood) vessels, cavities

Physical Measurements *in vivo*

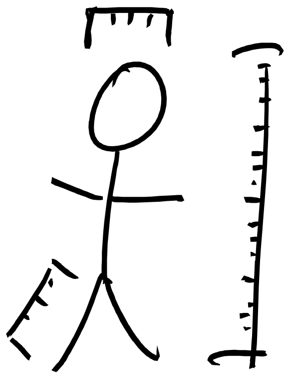

Outer body proportions:
length, height, width …

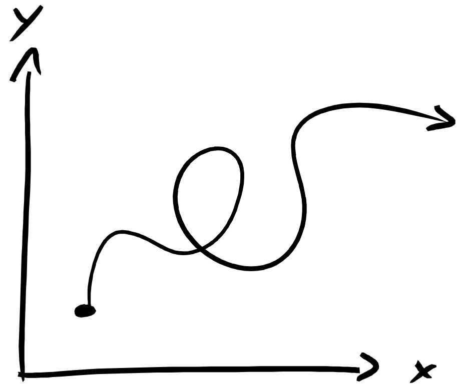

Kinematics (motion capturing)

Physical Measurements *in vivo*

MPI for Intelligent Systems (ps-old.is.tue.mpg.de)

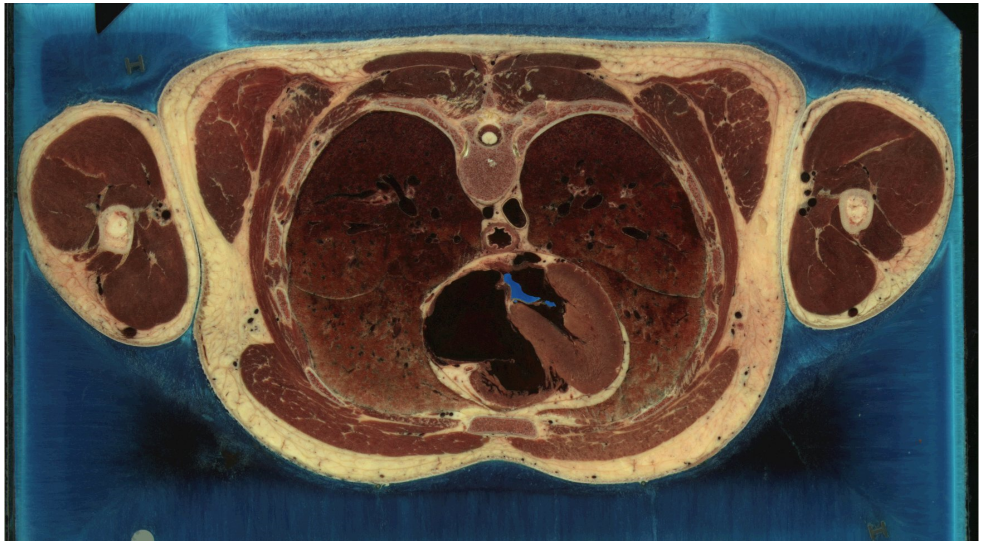

Visible Human Project

Introduction

Physical Measurements ex *vivo, in vitro*

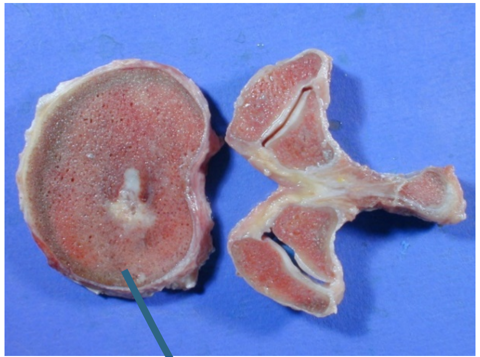

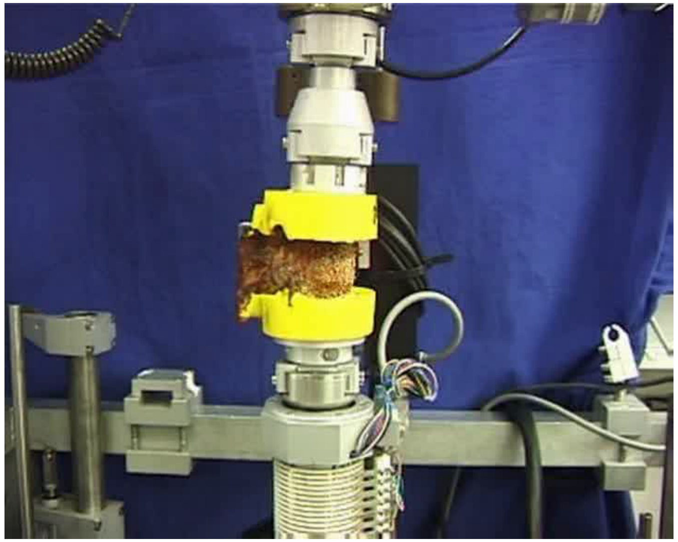

Scanning EM

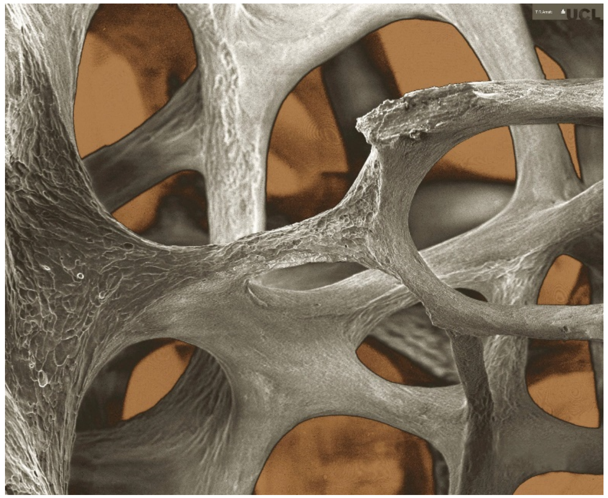

boneresearchsociety.org

Imaging Techniques

- Plethora of techniques: X-ray, EOS, CT, MRI, PET, SPECT, EIT, PAT, fPAM, fMRI, DW-MRI, thermography, endoscopy, …
- Invasive vs. non-invasive
- Anatomical vs. functional
- Projectional vs. tomographical
- Visible light vs. ionizing radiation vs. radio waves vs. sound waves vs. …
- Hard vs. soft tissue imaging
- Cheap vs. expensive

Non-Invasive Anatomical Imaging Techniques

Most widely used for comp. biomech. applications:

(X-ray) computed tomography (CT)

- Ionizing X-ray photons
- Excellent hard-tissue imaging

Magnetic resonance imaging

- Nuclear magnetic resonance, spin echo
- Excellent soft tissue imaging

Ultrasonography

- Ultrasonic/-sound waves (mechanical waves)
- Lower overall image quality, but „hazard-free“, real-time & inexpensive

X-Ray Physics Recap: Discovery

Wilhelm Conrad Röntgen (* 1845, † 1923)
Engineer & physicist

"Hand mit Ringen" (by W.C. Röntgen, 1895)

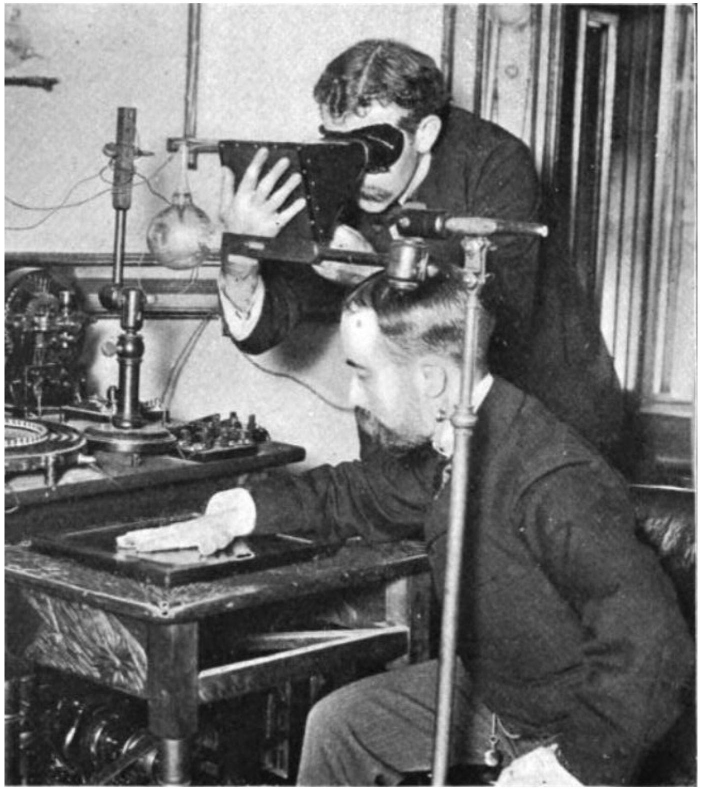

Morton & Hammer: The X-ray (1896)

Spectrum, Frequency & Energy

- High-energy photons: Ionizing, little absorption or scattering by soft tissue
- Planck-Einstein relation:
  $E = h\nu = h\frac{c}{\lambda}$
  - ν: photon frequency
  - h: Planck constant
  - c: speed of light (vacuum)
  - λ: photon wave length
- eV ("electronvolt"): kinetic energy of an elementary charge after passing 1 V of electric potential difference
  - $\approx 1.6 \cdot 10^{-19}$ J

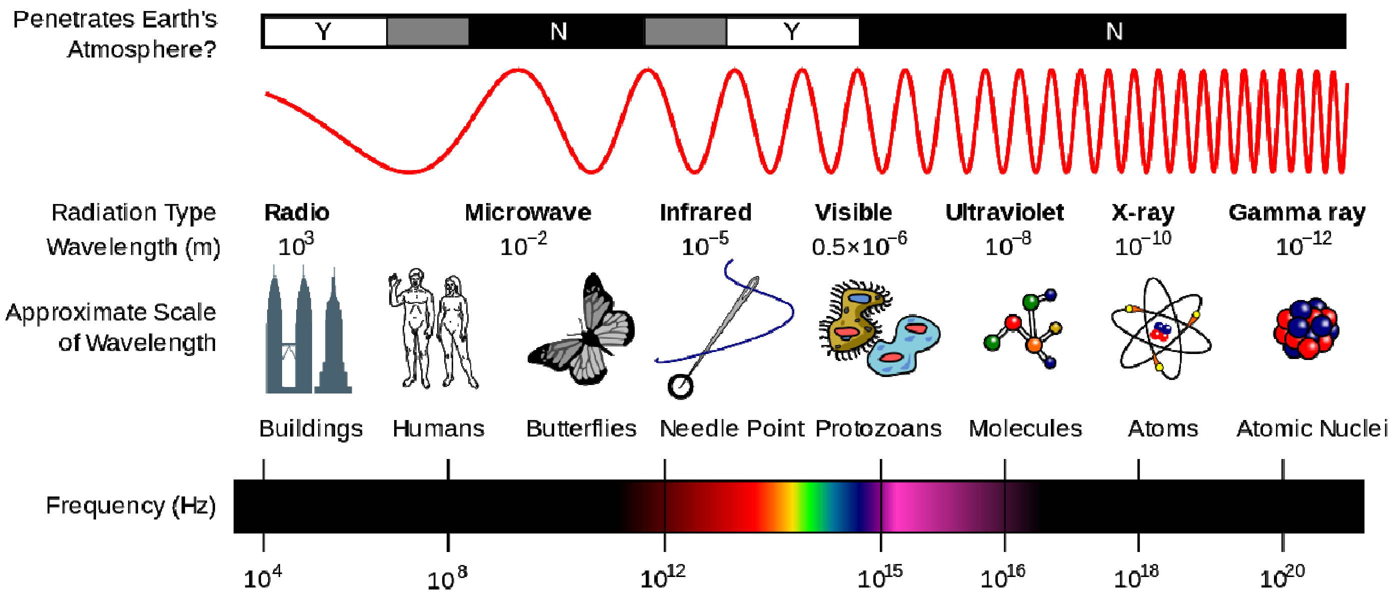

wikimedia.org

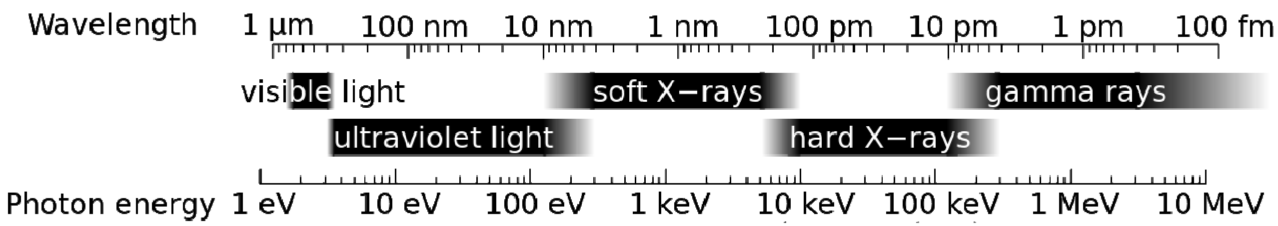

Interaction With Matter

Photoelectric effect

- X-ray photon transfers all its energy to an electron, ionizing the atom
- Outer electron fills gap, emits "characteristic photon" (~ orbital energy difference)*
- Dominant effect for bones

Compton scattering

- X-ray photon transfers fraction of its energy to outer or free electron
- Photon scattered in random direction, frequency reduced
- Dominant effect for soft tissues

Pair production

- X-ray photon near atomic nucleus converted to electron-positron pair
- Only relevant at *very* high energies (> 1.022 MeV = $2m_ec^2$, i.e. gamma ray region)

*or an "Auger electron"

+ Rayleigh scattering
+ Photodisintegration

Interaction With Matter

Photoelectric effect

- X-ray photon transfers all its energy to an electron,
-
-

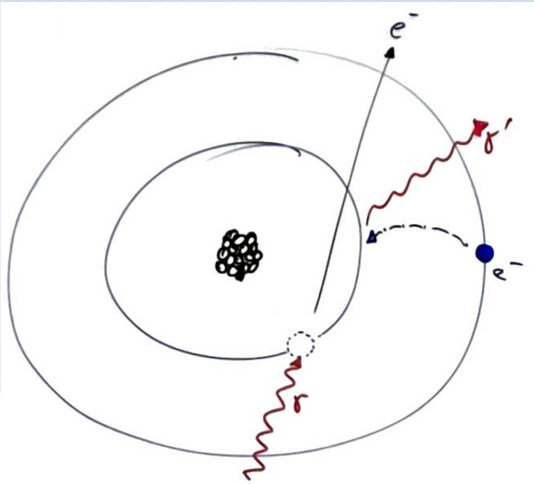

Compton scattering

- X-ray photon transfers fraction of its energy to outer or free electron
- Photon scattered in rand frequ
- Dom oft tissu

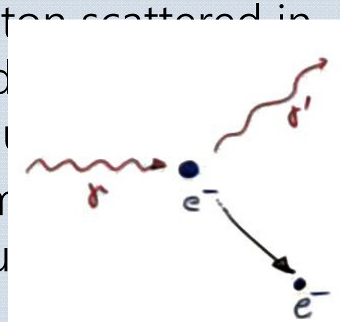

Pair production

- X-ray photon near atomic nucleus converted to electron-positron pair
- Only relevant at *very* high ener eV = $2m$ ay reg

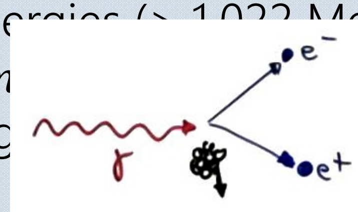

*or an "Auger electron"

+ Rayleigh scattering
+ Photodisintegration

Bulk Attenuation

Solving $\frac{d\Phi}{dx} = -n\sigma\Phi = -\mu\Phi = -(\mu_a + \mu_s)\Phi$

(1D radiative transfer, attenuation only)

yields Lambert-Beer law: $\Phi = \Phi_0 e^{-\mu x}$

Attenuation coefficient: $\mu \propto \rho \frac{Z^4}{E^3} = \rho \frac{Z^4}{(h\nu)^3}$

Mass attenuation coefficient: $\mu_\rho = \frac{\mu}{\rho} = \frac{n\sigma}{nm} = \frac{\sigma}{m}$

e.g. for $E = 40\ \mathrm{keV}$:

$\mu_{\rho,\mathrm{water}} \approx 0.27\ \mathrm{cm}^2/\mathrm{g}$
$\rho_{\mathrm{water}} = 0.99\ \mathrm{g/cm}^3$ $\Rightarrow \mu_{\mathrm{water}} \approx 0.27/\mathrm{cm}$

$\mu_{\rho,\mathrm{bone}} \approx 0.67\ \mathrm{cm}^2/\mathrm{g}$
$\rho_{\mathrm{bone}} = 1.85\ \mathrm{g/cm}^3$ $\Rightarrow \mu_{\mathrm{bone}} \approx 1.2/\mathrm{cm}$

http://www.nist.gov/pml/data/xraycoef/index.cfm

→ Tune energy for contrast

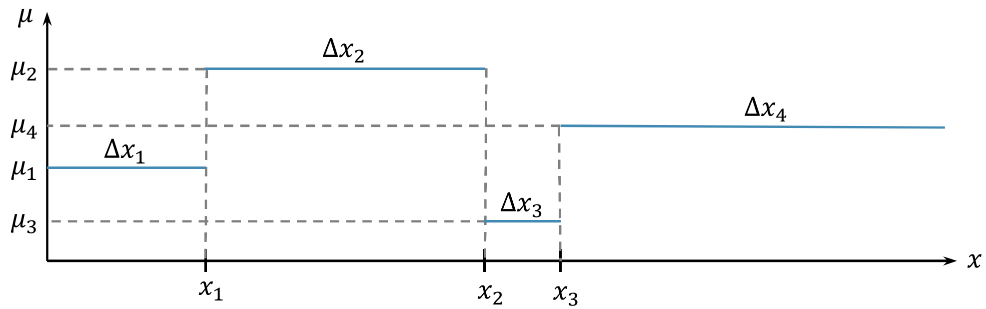

Non-constant μ: (piece-wise)

$$\Phi(x_1) = \Phi_0 e^{-\mu_1(x_1 - x_0)}$$
$$\Phi(x_2) = \Phi(x_1) e^{-\mu_2(x_2 - x_1)}$$
$$\vdots$$
$$\Phi(x_n) = \Phi(x_{n-1}) e^{-\mu_n(x_n - x_{n-1})}$$

With $\Delta x_i \coloneqq x_i - x_{i-1}$

$$\Rightarrow \Phi(x_n) = \Phi_0 \prod_{i=1}^{n} e^{-\mu_i \Delta x_i} = \Phi_0 e^{-\sum_{i=1}^{n} \mu_i \Delta x_i}$$

Let $\Delta x_i \to 0$

$$\Rightarrow \Phi(x_n) = \Phi_0 e^{-\int_0^{x_n} \mu(x)\, dx}$$

Φ: radiant flux (in W)
x: path traveled inside material (in m)
n: particle density (in $1/\mathrm{m}^3$)
m: particle mass (in kg)
ρ: mass density (in $\mathrm{kg/m}^3$)
σ: attenuation cross-section (in m^2)
μ: linear attenuation coefficient (in 1/m)
μ_a: absorption coefficient (in 1/m)
μ_s: scattering coefficient (in 1/m)
μ_ρ: mass attenuation coefficient (in m^2/kg)
Z: atomic number
E: X-ray energy

Generating X-Rays

- X-ray sources:
  - Astrophysical
  - Radioactive decay (γ decay)
  - X-ray vacuum tube
  - X-ray laser
  - Cyclic particle accelerators
- X-ray vacuum tube:
  - Hot cathode releases electrons
  - Acceleration by high-voltage electric field
  - Collision with metal anode → X-rays (1 %) + heat (99 %)
    - Characteristic X-ray radiation (spikes)
    - Bremsstrahlung (continuous)
  - Filter for beam hardening
- Detection: Scintillator + photo diode

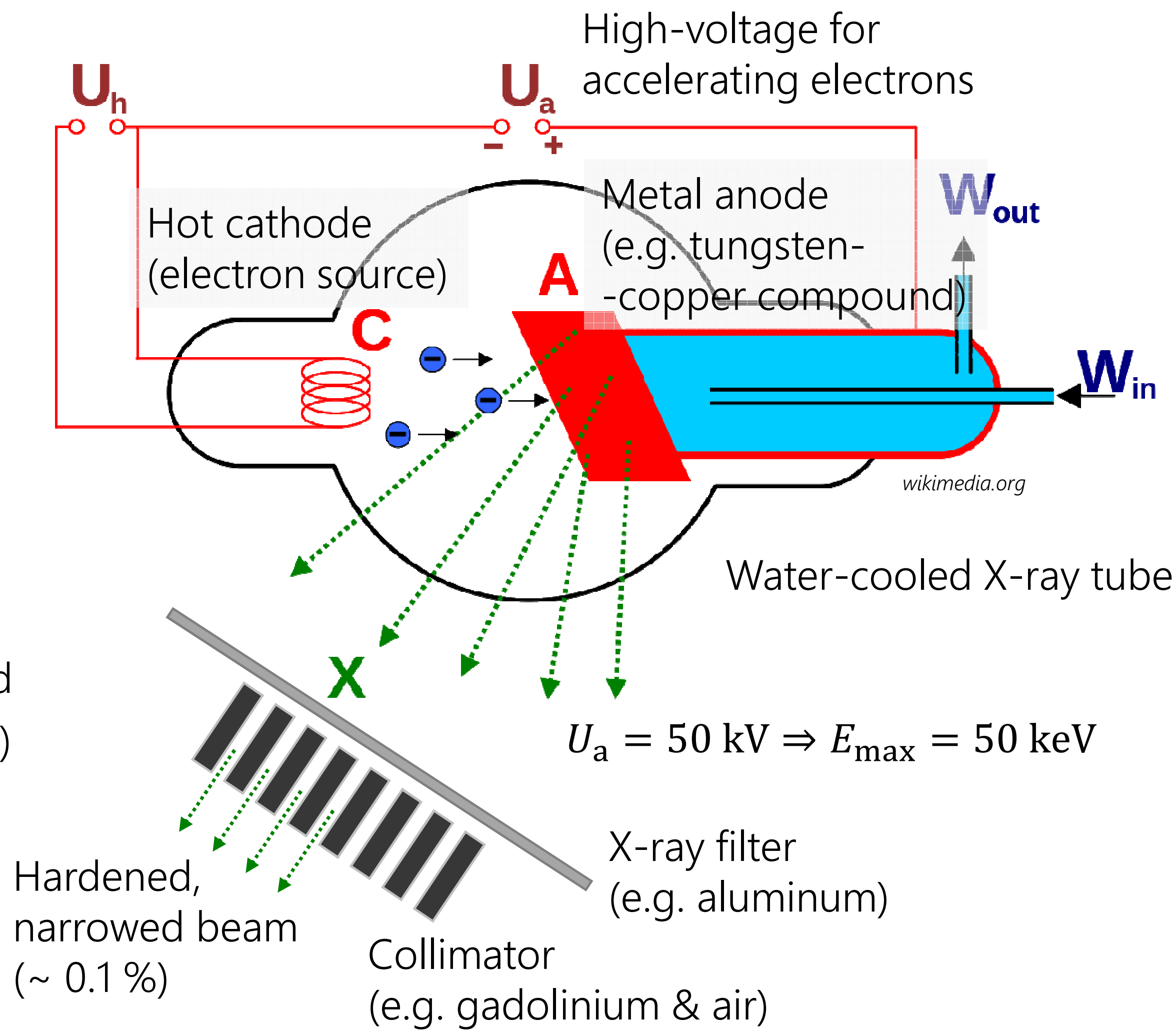

X-Ray CT Basics

- Process:
  - X-ray source rotates around subject
  - Detector on opposite side
  - After complete rotation, move subject axially
  - Repeat
- Properties:
  - Tomographical
  - High contrast
  - Sub-mm resolution
  - High radiation dosage (100 – 1000× proj. X-ray)
  - Requires contrast agent for soft-tissue imaging
  - Output: raw data (projections) must be post-processed, yielding a stack of 2D slices
- Modern devices: spiral/helical CT, multi-slice CTs
  - Reduced scan times
  - Reduced motion artefacts

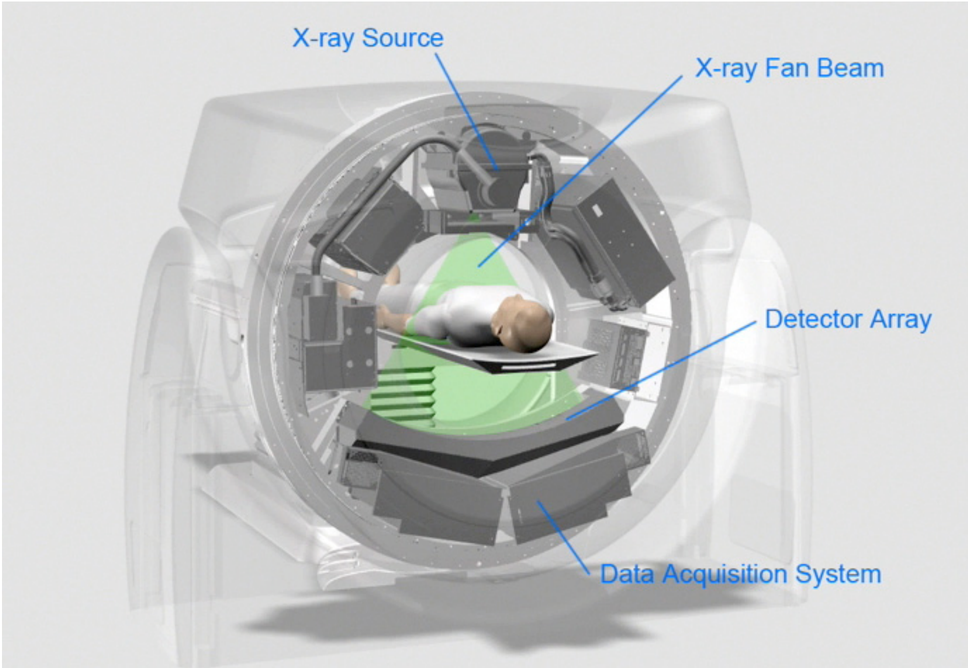

Projection

For some ray (x, θ) the X-ray detector receives

$$\Phi(x', \theta) = \Phi_0 \exp \int_{-\infty}^{+\infty} \mu(x, y)\, dy'$$

with

$$x = x' \cos\theta - y' \sin\theta$$
$$y = x' \sin\theta + y' \cos\theta$$

Note that

$$\mathcal{R}_\theta(\mu)(x') = \int_{-\infty}^{+\infty} \mu(x, y)\, dy' = -\ln\left(\frac{\Phi(x', \theta)}{\Phi_0}\right)$$

is the **Radon transform** of μ.

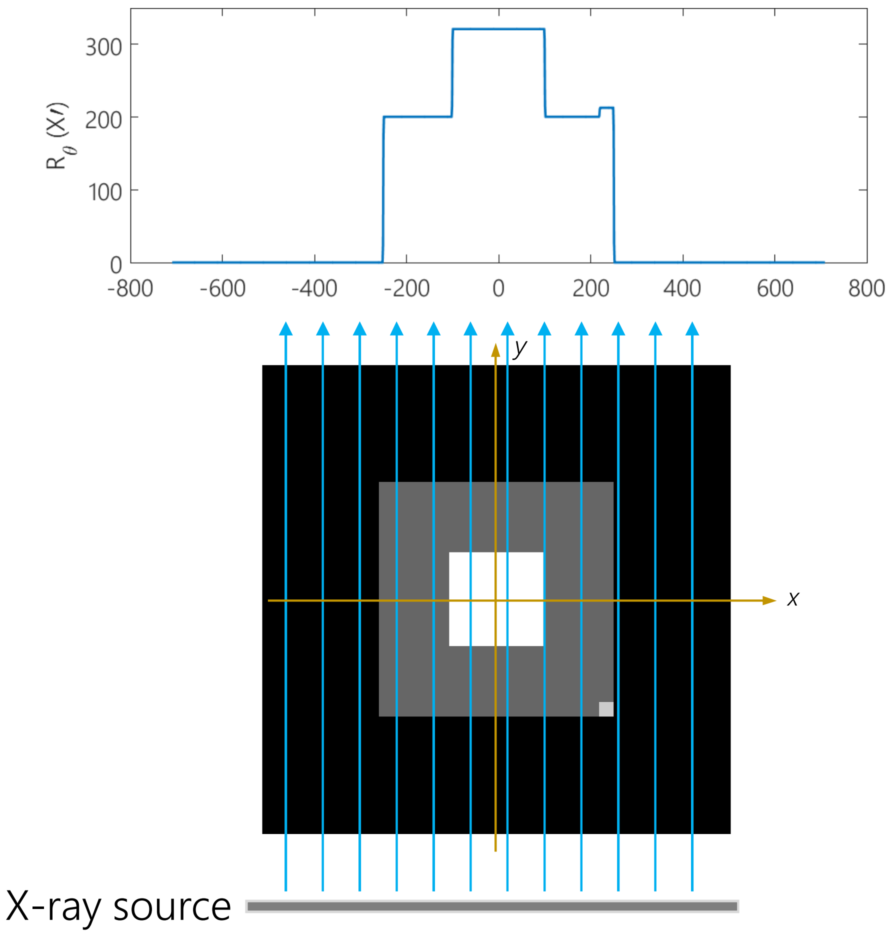

Projection

For some ray (x, θ) the X-ray detector receives

$$\Phi(x', \theta) = \Phi_0 \exp \int_{-\infty}^{+\infty} \mu(x, y)\, dy'$$

with

$$x = x' \cos\theta - y' \sin\theta$$
$$y = x' \sin\theta + y' \cos\theta$$

Note that

$$\mathcal{R}_\theta(\mu)(x') = \int_{-\infty}^{+\infty} \mu(x, y)\, dy' = -\ln\left(\frac{\Phi(x', \theta)}{\Phi_0}\right)$$

is the **Radon transform** of μ.

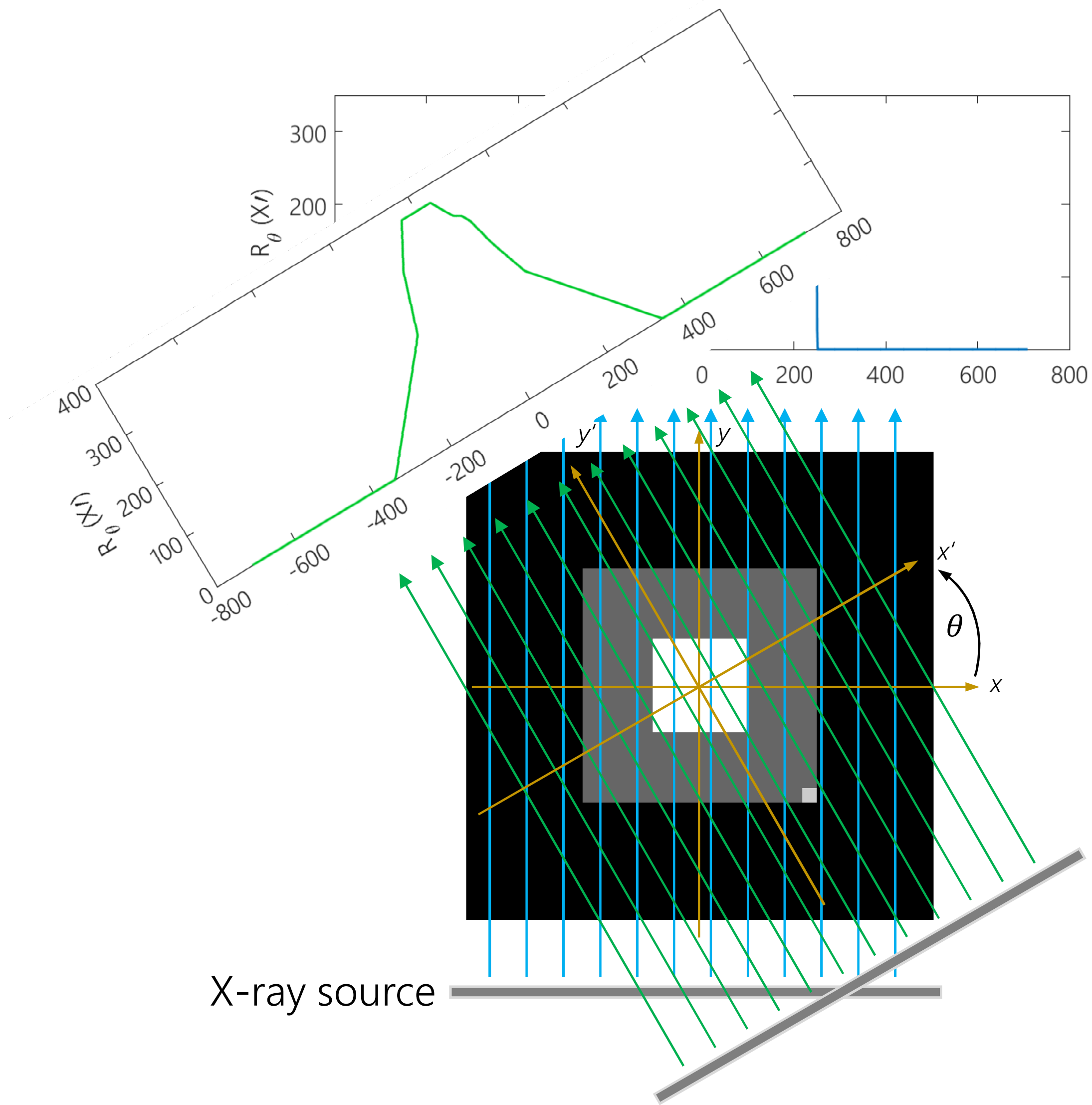

Projection

For some ray (x, θ) the X-ray detector receives

$$\Phi(x', \theta) = \Phi_0 \exp \int_{-\infty}^{+\infty} \mu(x, y)\, dy'$$

with

$$x = x' \cos\theta - y' \sin\theta$$
$$y = x' \sin\theta + y' \cos\theta$$

Note that

$$\mathcal{R}_\theta(\mu)(x') = \int_{-\infty}^{+\infty} \mu(x, y)\, dy' = -\ln\left(\frac{\Phi(x', \theta)}{\Phi_0}\right)$$

is the **Radon transform** of μ.

Repeat for [0°, 180°) → sinogram:

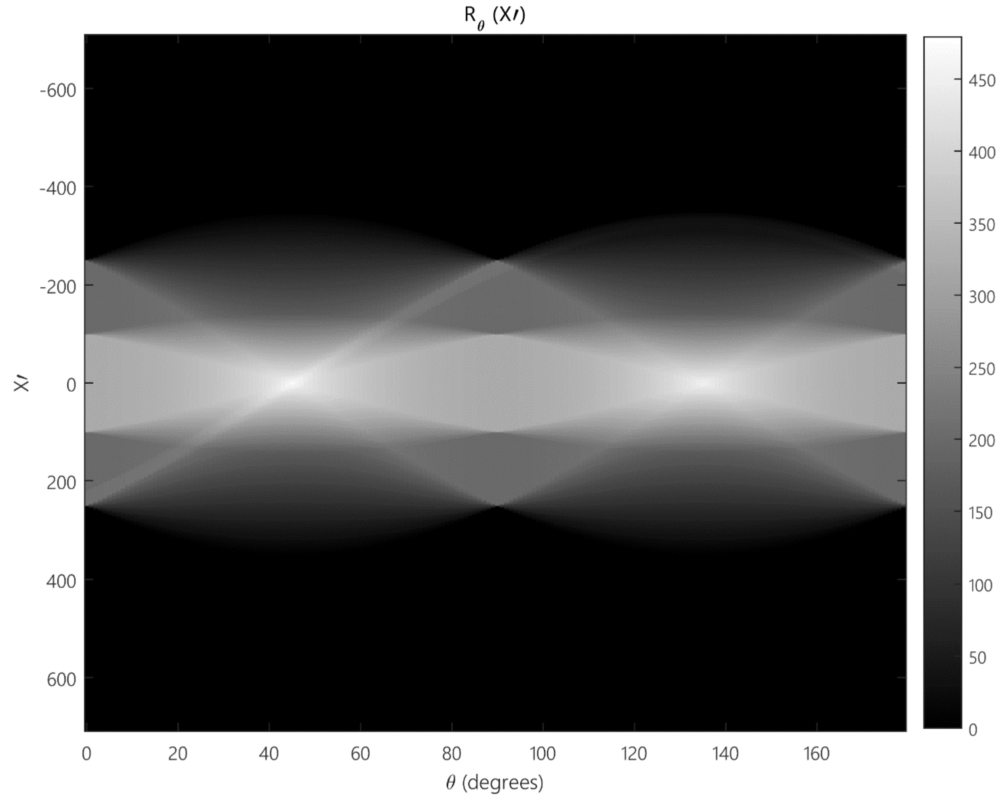

Back-Projection

Reconstruct μ by inverting the Radon transform

$$\mu(x, y) = \frac{1}{\pi} \int_0^{\pi} \mathcal{R}_\theta(\mu)(x \sin\theta + y \cos\theta)\, d\theta$$

Back-Projection: "smear" line integral values along projection paths, averaging contribution of different angles per pixel

But: That actually constructs

$$\tilde{\mu}(x, y) = \frac{1}{\|\boldsymbol{x}\|} * \mu(x, y)$$

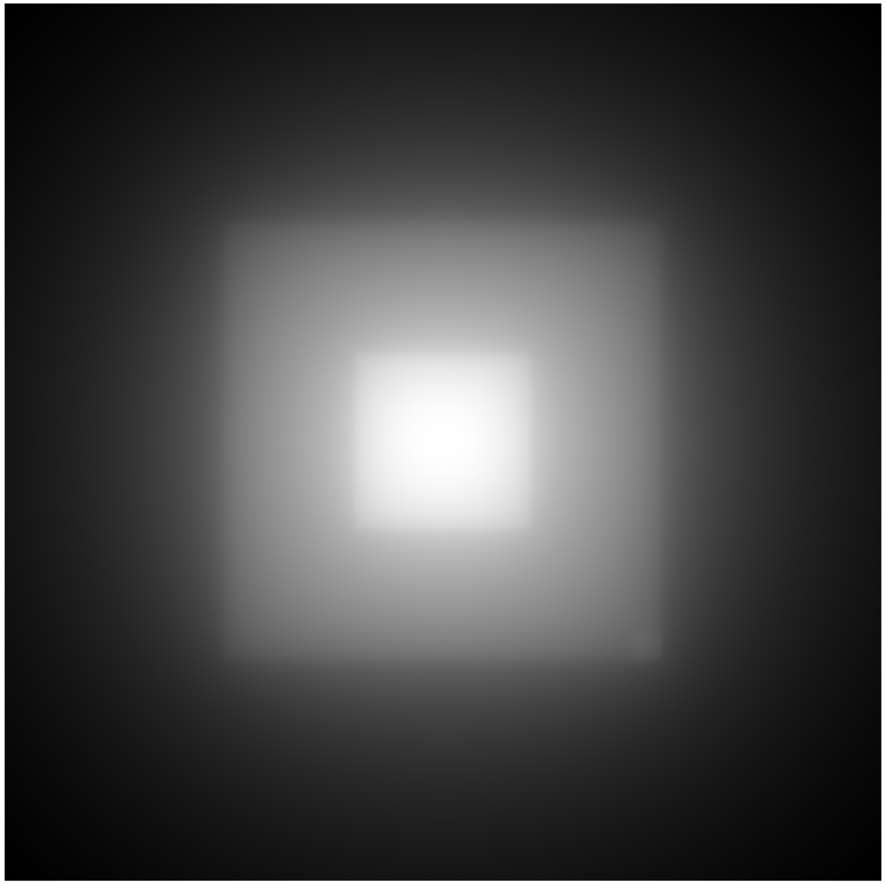

Fourier Reconstruction

Fourier slice theorem

$$\mathcal{F}_1\mathcal{R}_\theta(\mu) \equiv \mathcal{S}_\theta\mathcal{F}_2(\mu)$$

- Fourier transform of projection along θ = slice under θ through 2D frequency space

- Fourier reconstruction: Reconstruct $\mathcal{F}_2(\mu)$ from 1D Fourier-transformed projections
- Apply inverse Fourier transform to reconstruct image

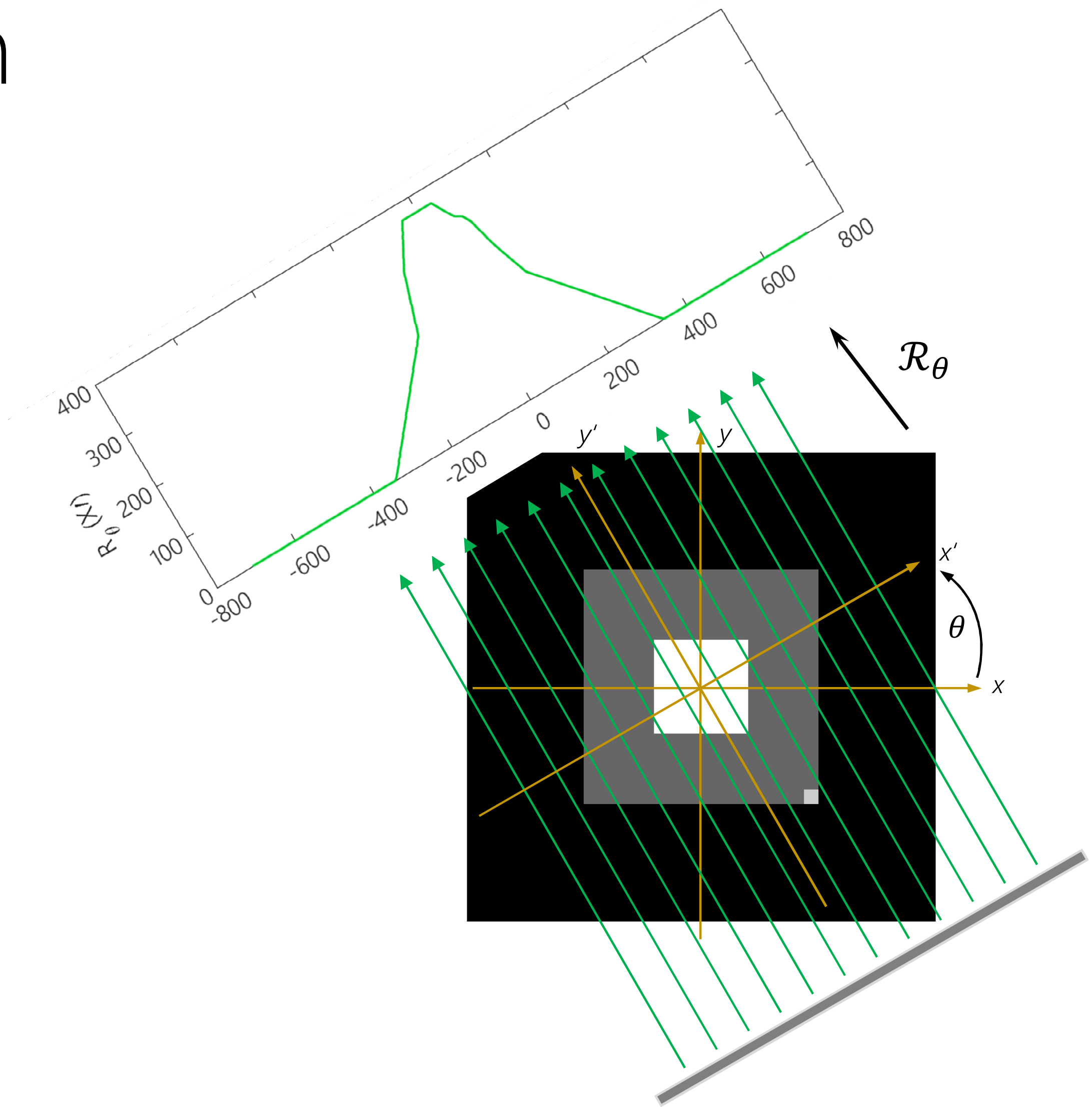

Imagi

Fo

Fourie

- Fourier transform of projection along θ = slice under θ through 2D frequency space

- F … om
  1

- A … ct
  i

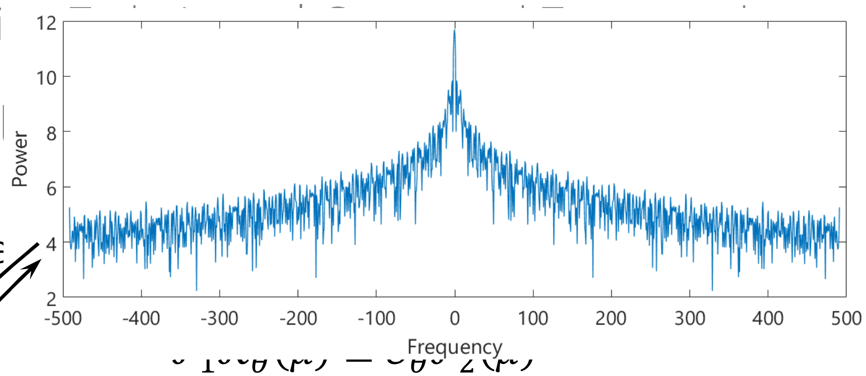

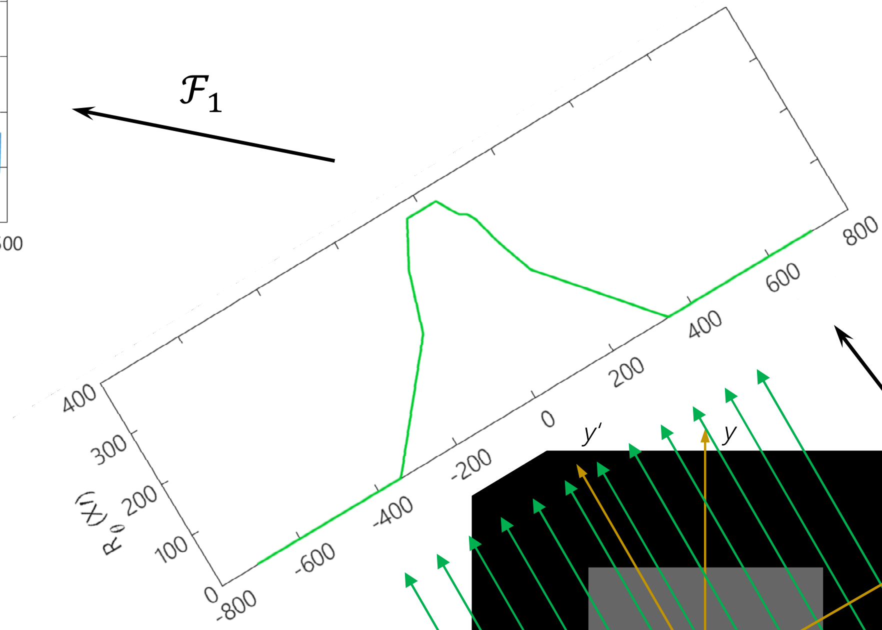

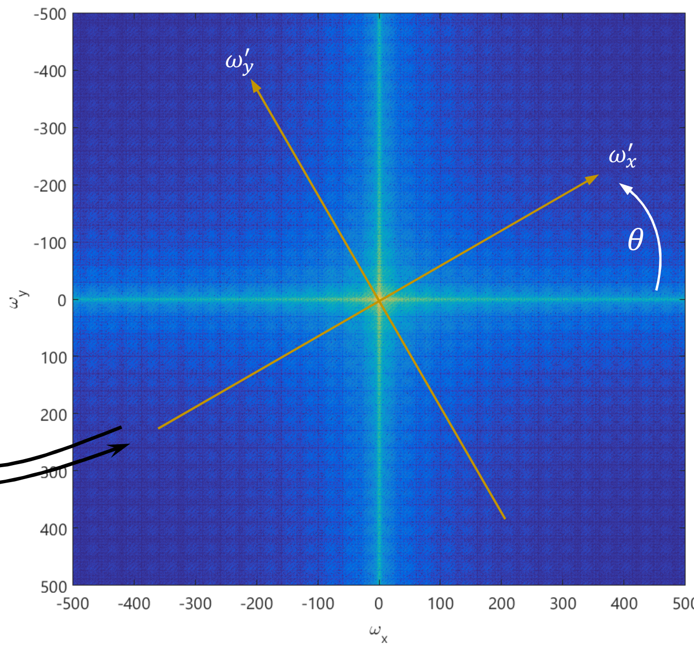

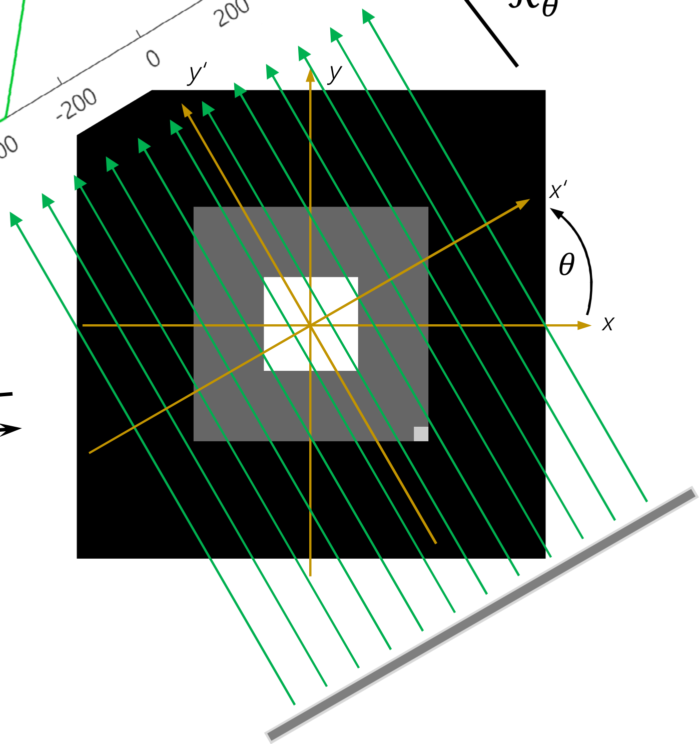

Filtered Back-Projection

- Filtered Back-Projection: back-project high-pass filtered sonogram (→ cf. Fourier slice theorem)

$$\mu(x, y) \approx \frac{1}{\pi} \int_0^\pi \mathcal{F}_1^{-1}\big(|\omega_x'|\, \mathcal{F}_1 \mathcal{R}_\theta(\mu)\big)(x \sin\theta + y \cos\theta)\, d\theta$$

- Naïve high-pass also amplifies noise
- Alternatives: Iterative techniques (e.g. Algebraic Reconstruction Technique, ART et al.)

$$\mathcal{R}_{\theta_i}(\mu)(x_i{}') = \sum_j P_{ij}\mu(x_i, y_i)$$

$$\boldsymbol{r} = \boldsymbol{P}\boldsymbol{m} \Rightarrow \boldsymbol{m} = \boldsymbol{P}^{-1}\boldsymbol{r}$$

- Statistical noise models (MBIR), EM algorithms …
- Fan- and cone-beam geometry requires special treatment

$\Delta\theta = 1.0°$

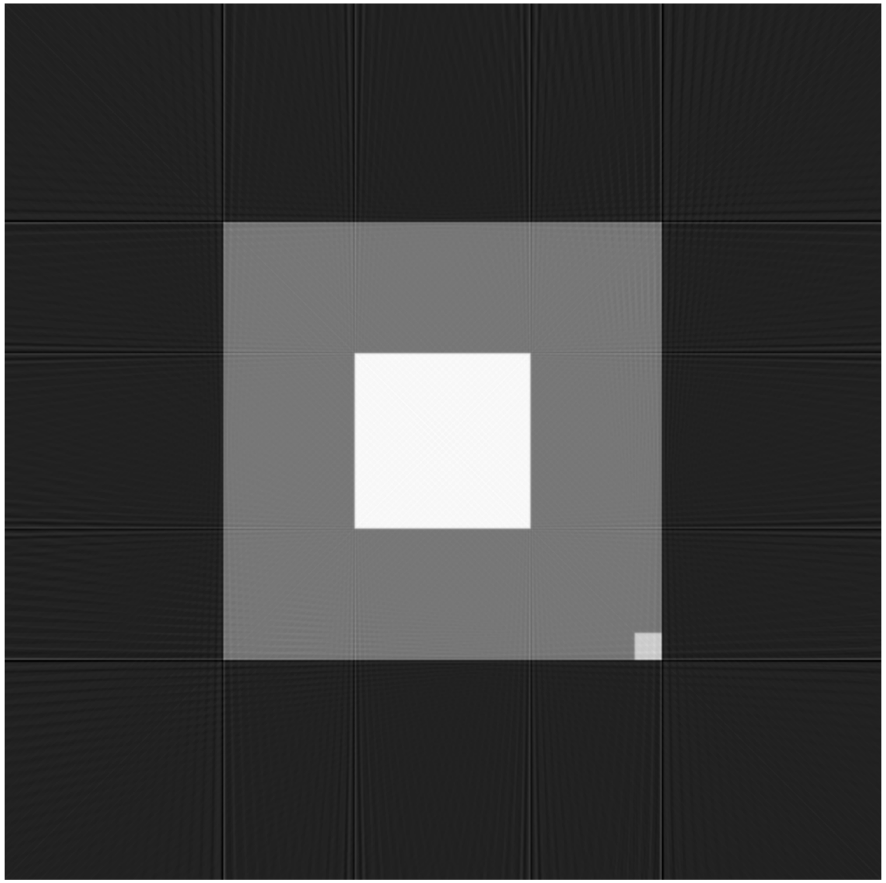

+ Hamming-windowed Ram-Lak filter

Hounsfield Scale

- Radiodensity depends on scan parameters
- Normalize measured attenuation to attenuation rate of water and air
  - Hounsfield units $HU(\mu) \coloneqq 1000 \frac{\mu - \mu_{\text{water}}}{\mu_{\text{water}} - \mu_{\text{air}}}$
  - $HU(\mu_{air}) = -1000$, $HU(\mu_{\text{water}}) = 0$
  - A.k.a. "CT numbers"
- Every tissue type has a specific HU range
- Windowing: compress full high-dynamic range signal to displayable range
- QCT (quantitative CT): calibrated with phantom to map HU to BMD (bone mineral density)

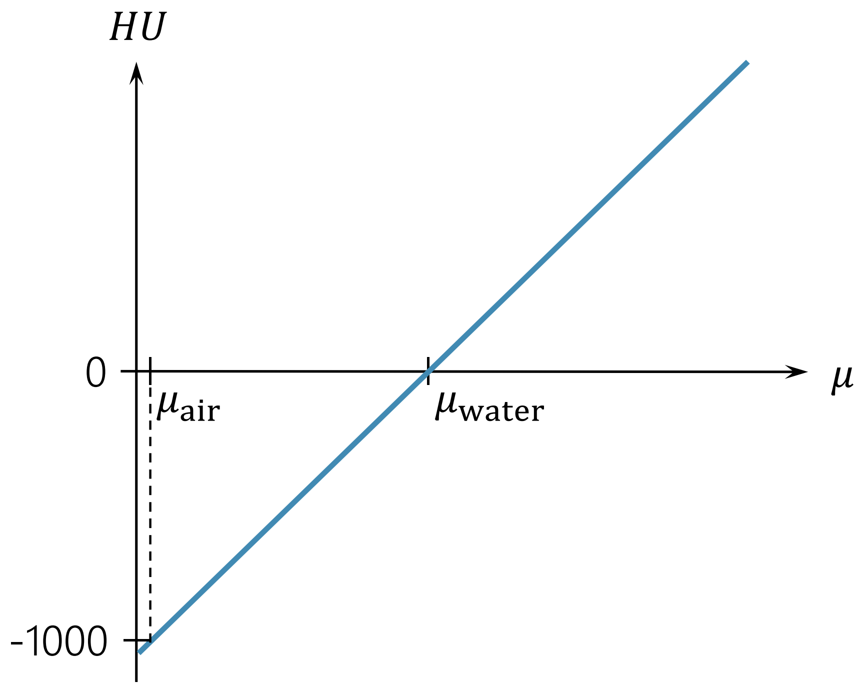

pQCT phantoms

Example

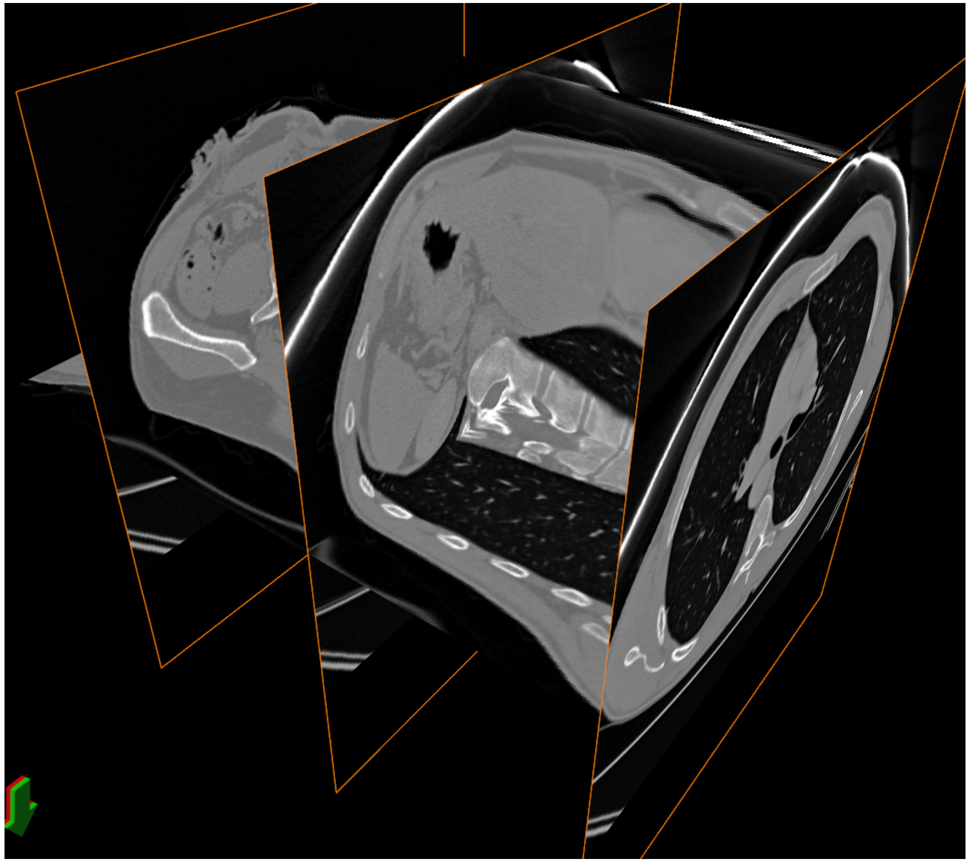

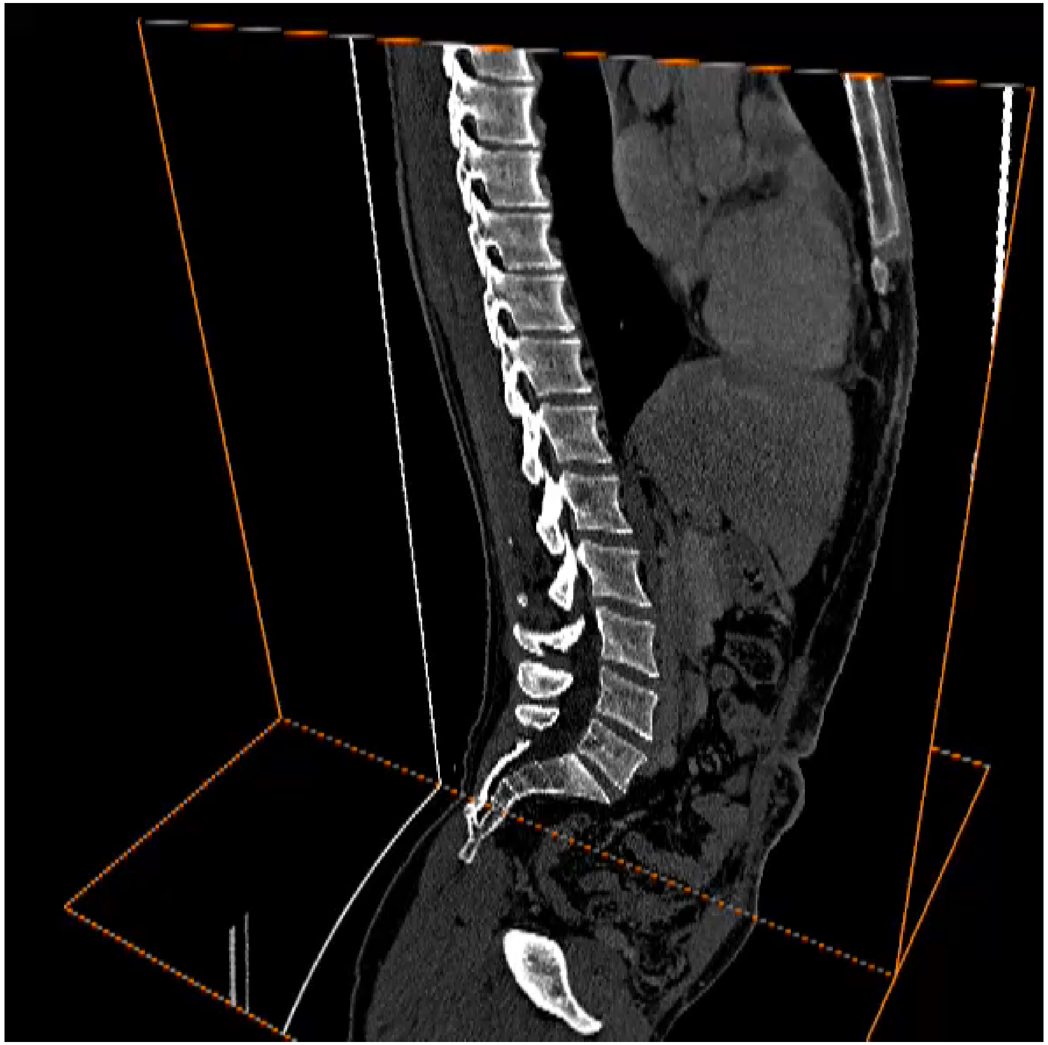

Example

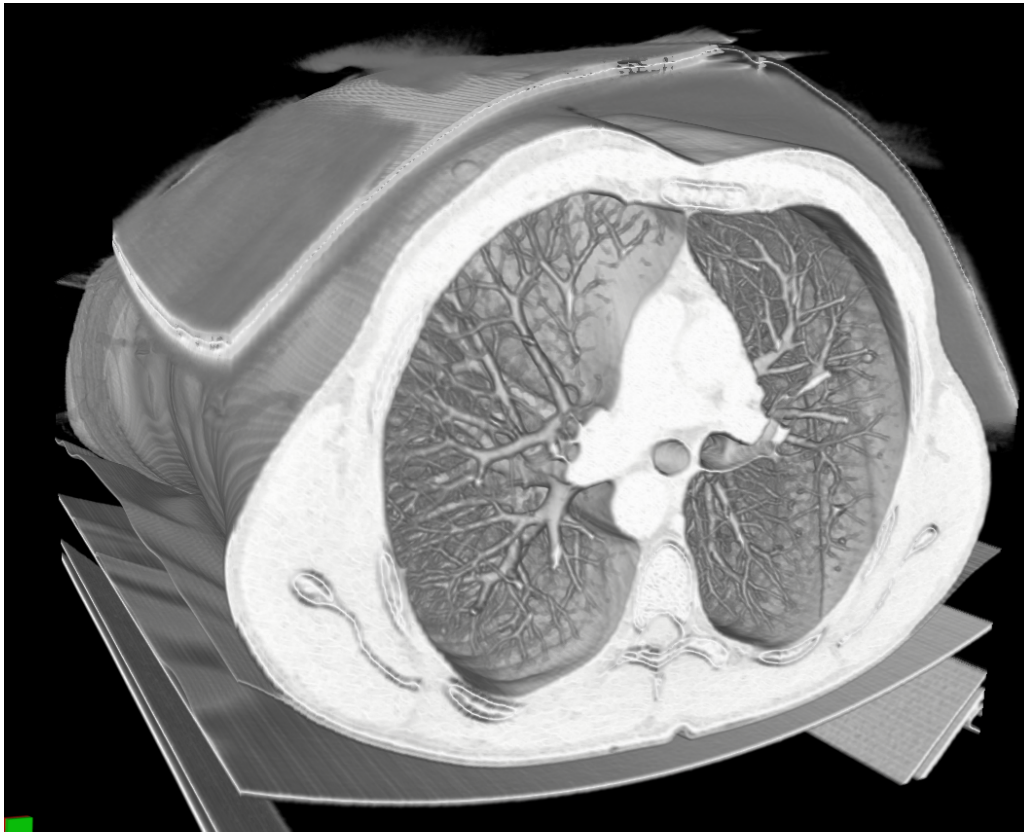

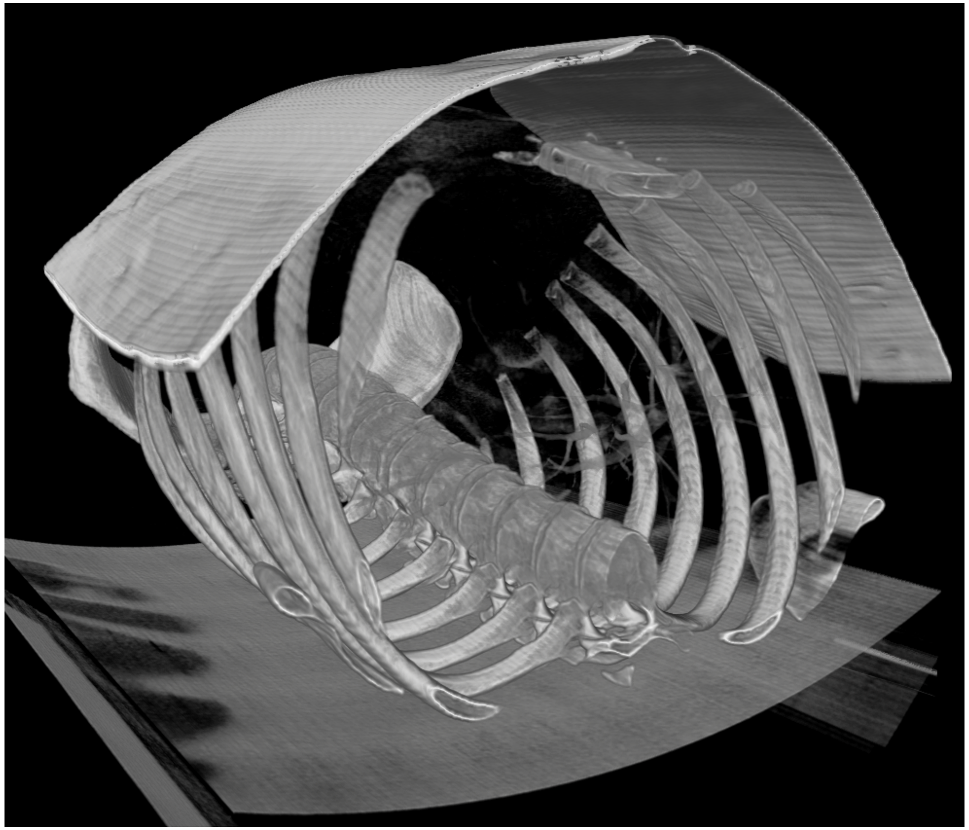

Computed Micro-Tomography (µCT)

- High-resolution CT (< 10 µm)
- Typically …
  - In vitro only (long scan times, high radiation doses, lethal for small animals)
  - Cone-beam (2D sensor) instead of fan-beam
  - Specimen is rotated
  - Small samples only

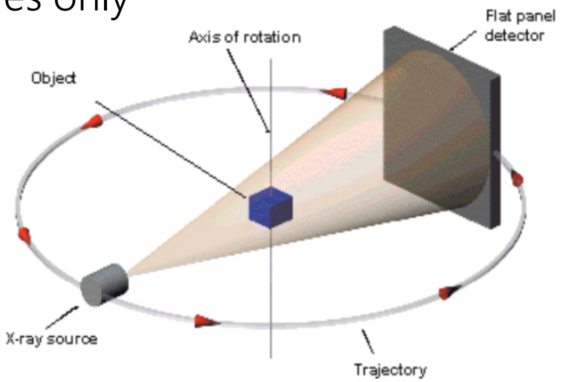


Sheep, CT

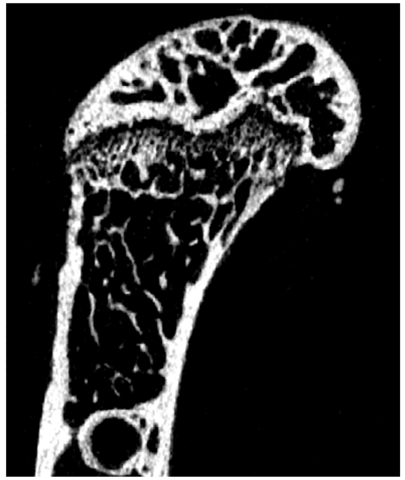
Mouse, µCT

Non-Invasive Anatomical Imaging Techniques

Most widely used for comp. biomech. applications:

(X-ray) computed tomography (CT)

- Ionizing X-ray photons
- Excellent hard-tissue imaging

Magnetic resonance imaging

- Nuclear magnetic resonance, spin echo
- Excellent soft tissue imaging

Ultrasonography

- Ultrasonic/-sound waves (mechanical waves)
- Lower overall image quality, but „hazard-free“, real-time & inexpensive

Magnetic Resonance Imaging (MRI)

- Basic receipe:
  1. Put subject into strong magnetic field
  2. Wait
  3. Transmit short radio pulse (~ 30 ms)
  4. Receive radio waves from subject (10 – 100 ms)
  5. Repeat 3. and 4. a number of times
  6. Use inverse Fourier transform to reconstruct image
- Strong, static field (primary field, $\boldsymbol{B_0}$)
  - Typically 1.5 – 3 T, up to 7 T
  - Superconducting magnets, liquid helium-cooled
- HF field/pulse ($\boldsymbol{B_1}$ perpendicular to $\boldsymbol{B_0}$)
  - Radio frequency (RF, MHz-range)
- Gradient fields (vary spatially and/or temporally)

wikimedia.org

Magnetic Resonance Imaging (MRI)

- Basic receipe:
  1. Put subject into s
  2. Wait
  3. Transmit short ra
  4. Receive radio wa
  5. Repeat 3. and 4.
  6. Use inverse Four
- Strong, static field (
  - Typically 1.5 – 3 T
  - Superconducting
- HF field/pulse ($\boldsymbol{B}_1$ perpendicular to $\boldsymbol{B}_0$)
  - Radio frequency (RF, MHz-range)
- Gradient fields (vary spatially and/or temporally)

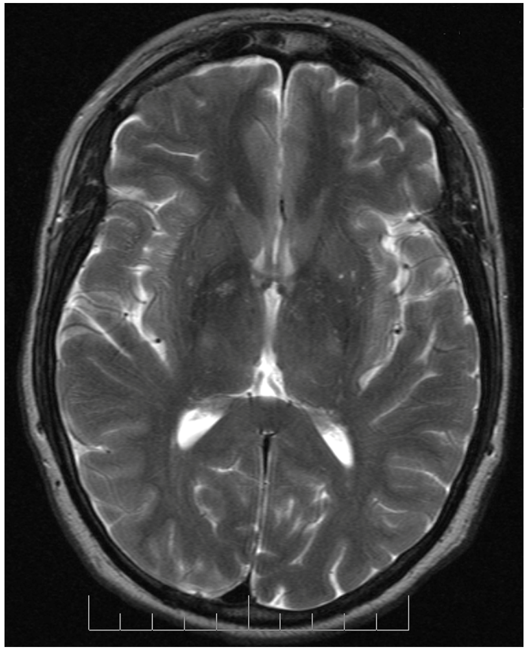

wikimedia.org

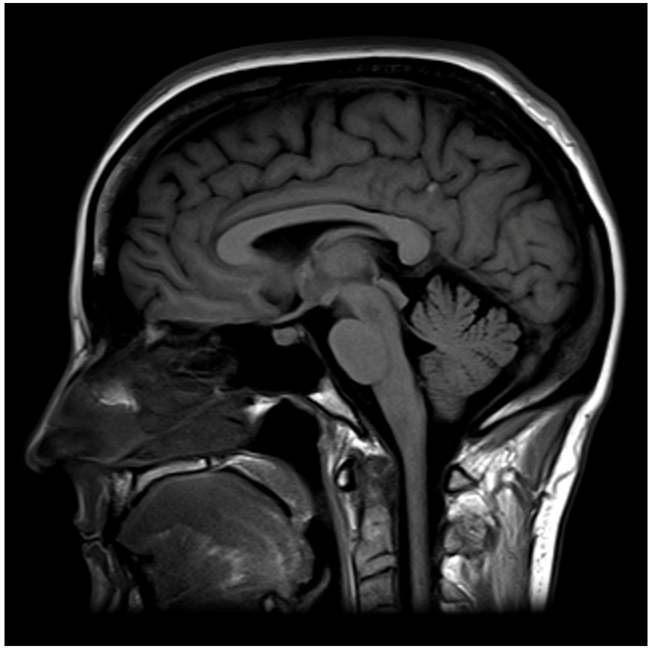

radiopedia.org

wikimedia.org

Discovery of NMR & Invention of MRI

- Based on nuclear magnetic resonance (NMR)
  - Nuclei in a magnetic field absorb an re-emit RF energy, verified in the 50s, 1952 Nobel Prize in physics
  - NMR in condensed matter discovered independently by Edward Purcell et al. and Felix Bloch et al. (1946)
  - Preliminary work: Zeeman 1896, Planck 1899/1900, Einstein 1905, Sommerfeld 1916, Stern & Gerlach 1922, Rabi 1936
- 1960s: NMR spectroscopy
- Raymond Damadian 1971: Cancer cells have different NMR properties than normal tissue (patent filed 1972)
- 1971: MRI imaging via field-gradient NMR invented by Paul Lauterbur & Peter Mansfield (Nobel Prize in Medicine 2003)
- 1977: First clinical images (Lauterbur, Mannsfield, Damadian)

Raymond Damadian (left) with assistant Larry Minkoff (right)

Early Milestones

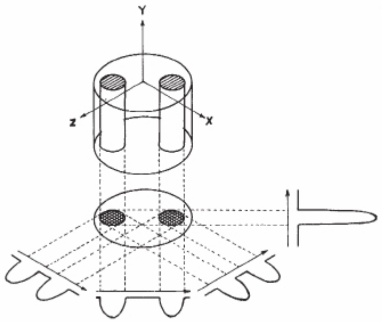

Fig. 1 Relationship between a three-dimensional object, its two-dimensional projection along the Y-axis, and four one-dimensional projections at 45° intervals in the XZ-plane. The arrows indicate the gradient directions.

Fig. 2 Proton nuclear magnetic resonance zeugmatogram of the object described in the text, using four relative orientations of object and gradients as diagrammed in Fig. 1.

Projectional NMR tomography
(Lauterbur 1973)

Medical imaging by NMR

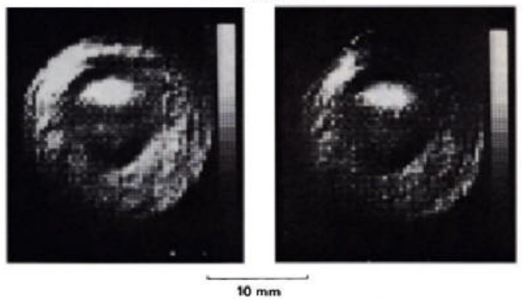

Fig. 4.
Cross-sectional images of a finger obtained *in vivo* by NMR (see text for full details).
(A) delay τ = 0.5 sec, (B) delay τ = 0.3 sec.

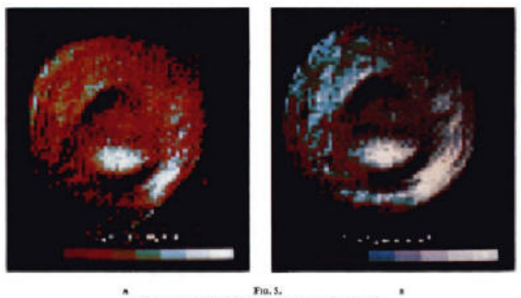

Fig. 5.
Colour versions of the finger images shown in Figs. 4A and B.
(A) The eight colours black through to white correspond to data levels 6–13. The delay time τ = 0.5 sec.
(B) The eight colours black through to white correspond to data levels 2–9.
In both pictures, data falling outside the window limits are presented as all black or all white as appropriate.

Scan of a human finger via
gradient-field slice selection
(Mansfield & Maudsley 1977)

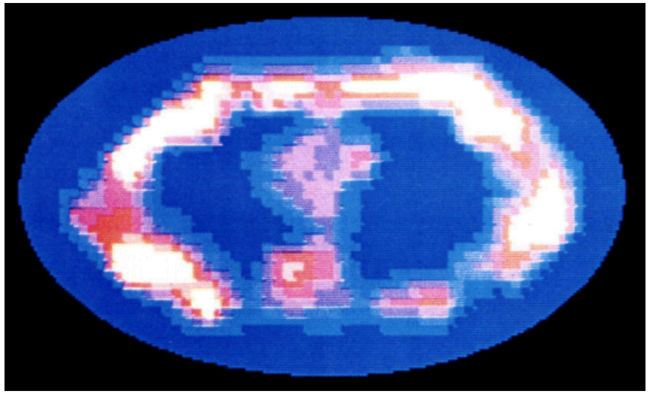

First scan of live human being (chest)
Scan time: ~ 5 hours ("field-focused MRI")
(Damadian, 1977)

Polarization (Magnetization)

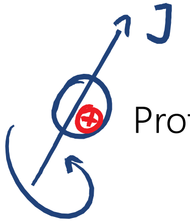

Angular momentum

Proton

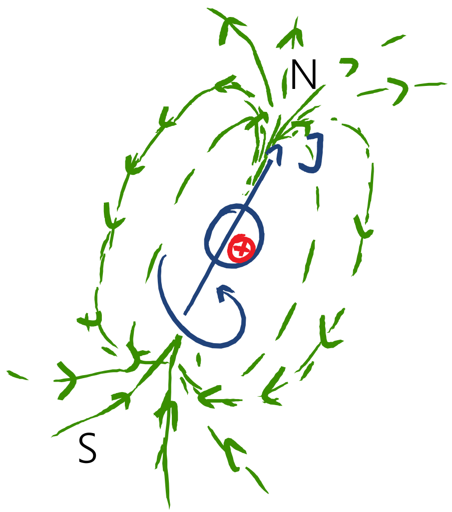

Magnetic moment

$\boldsymbol{\mu} = \gamma \boldsymbol{J} \Rightarrow \boldsymbol{\tau} = \boldsymbol{\mu} \times \boldsymbol{B_0}$

Without external field: “degenerate”, no net magnetization

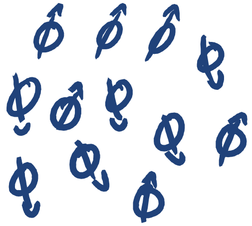

With external field:
spin-up : spin-down > 1*

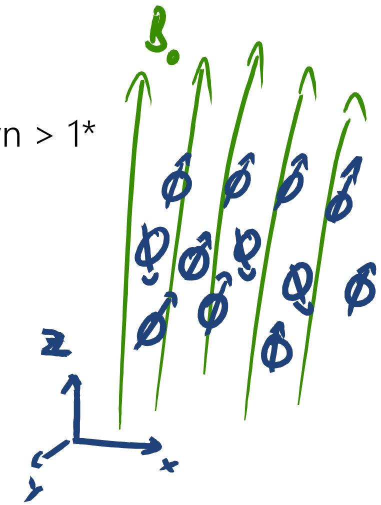

Larmor frequency $f_{\mathrm{L}} = \frac{\gamma}{2\pi} B_0$

Gyromagnetic ratio $\gamma = 42.58\ \mathrm{MHz/T}$

Potential energy due to alignment in B-field:

$$E = -(\boldsymbol{\mu} \cdot \boldsymbol{B_0}) \equiv -mh\frac{\gamma}{2\pi}B_0 = -mhf_{\mathrm{L}}$$

$\Rightarrow$ $m = 1/2$ is lower energy state (“parallel” to $\boldsymbol{B_0}$)

$\Rightarrow$ Energy difference between eigenstates $\Delta E = hf_{\mathrm{L}}$

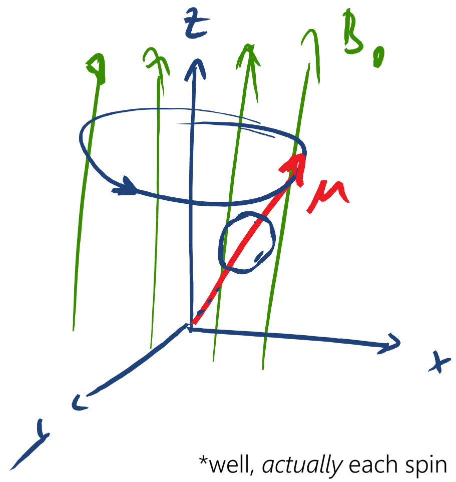

*well, *actually* each spin is a linear combination of spin-up/-down (superposition)…

Excitation

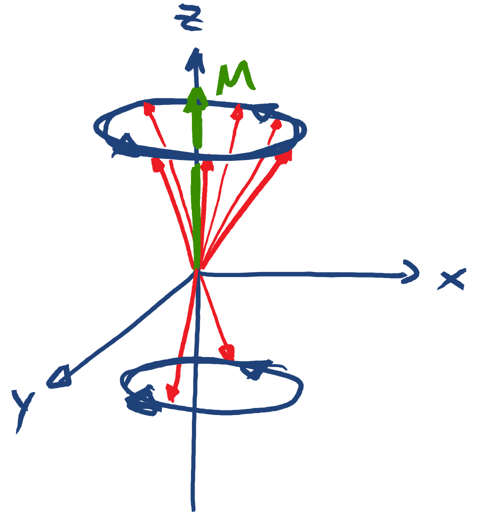

Spin state after polarization of some volume dV

$\boldsymbol{M} = d\overline{\boldsymbol{\mu}}/dV$: net (macroscopic) magnetization

Excess „up" states: ~ 9 ppm @ 1.5 T

$\frac{\pi}{2}$ pulse @ f_{L}

$\boldsymbol{B_1} \perp \boldsymbol{B_0}$

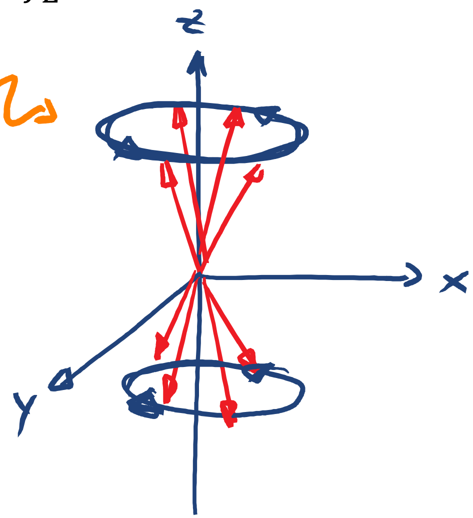

Some nuclei switch energy levels

→ decreased longitudinal magnetization

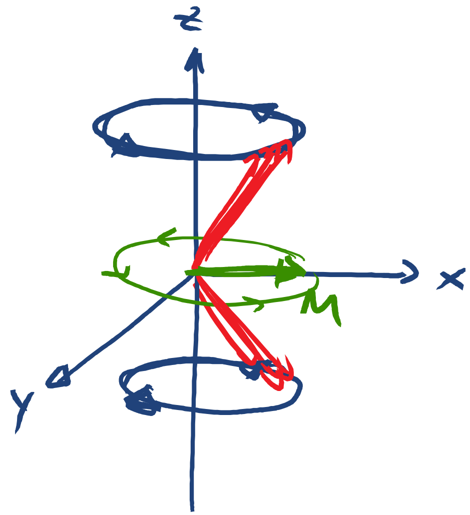

Phase coherence

("synchronized precession", actually an asymmetry of transverse components of angular momentum)

→ increased transversal magnetization

Relaxation

- Longitudinal relaxation (“spin-lattice relaxation”):
  - Nuclei return to low energy states (thermal equilibrium distribution)
  - Energy (heat) transferred to surroundings (lattice)
  - T_1: time to recover 63 % of longitudinal magnetization (~1 s for soft tissues)
- Transversal relaxation (“spin-spin relaxation”):
  - Phase decoherence over short time
  - Caused by inhomogeneities of the local magnetic fields
  - T_2: time for transversal magnetization to decay to 37 % (~ 10 … 50 ms for soft tissues)
- $T_1 < T_2$
- Net magnetization “spirals”, induces current in receiver coil → Free Induction Decay (FID)

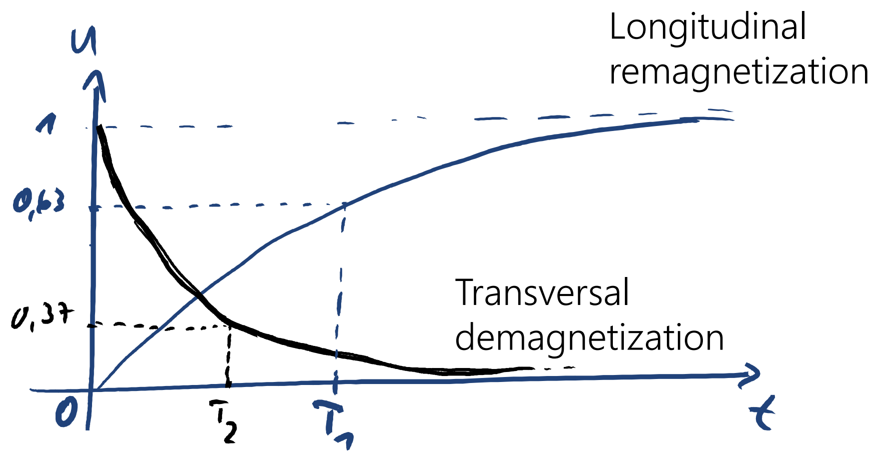

Bloch equations:

$$\dot{M}_x(t) = \gamma \cdot (\boldsymbol{M}(t) \times \boldsymbol{B_0})_x - \frac{M_x(t)}{T_2}$$

$$\dot{M}_y(t) = \gamma \cdot (\boldsymbol{M}(t) \times \boldsymbol{B_0})_y - \frac{M_y(t)}{T_2}$$

$$\dot{M}_z(t) = \gamma \cdot (\boldsymbol{M}(t) \times \boldsymbol{B_0})_z - \frac{M_z(t) - M_0}{T_1}$$

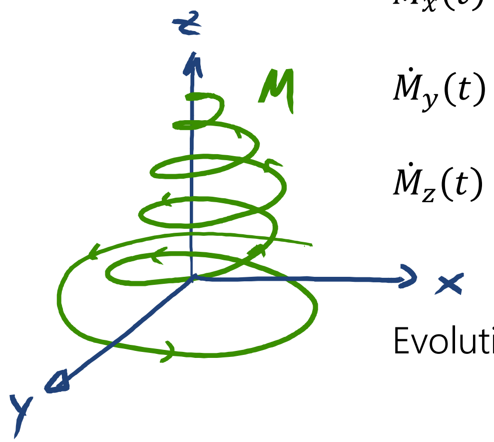

Evolution of net magnetization

Relaxation Times @ 1.5 T

Tissue type	Approximate T_1 value in ms	Approximate T_2 value in ms
Adipose tissues	240 – 250	60 – 80
Whole blood (deoxygenated)	1350	50
Whole blood (oxygenated)	1350	200
Cerebrospinal fluid (similar to pure water)	4200 – 4500	2100 – 2300
Gray matter of cerebrum	920	100
White matter of cerebrum	780	90
Liver	490	40
Kidneys	650	60 – 75
Muscles	860 – 900	50

https://en.wikipedia.org/wiki/Relaxation_%28NMR%29

Projection Reconstruction

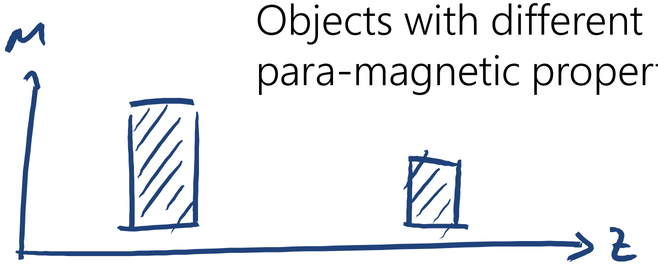

Objects with different
para-magnetic properties

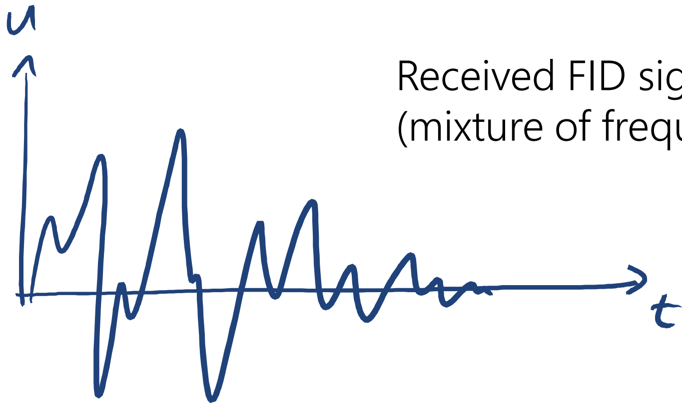

Received FID signal
(mixture of frequencies)

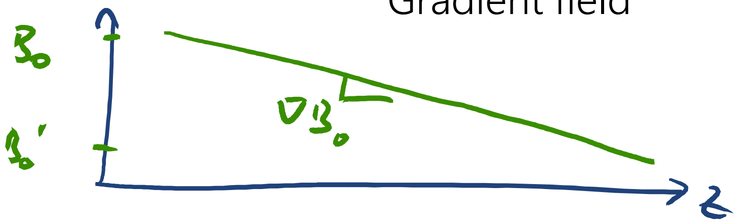

Gradient field

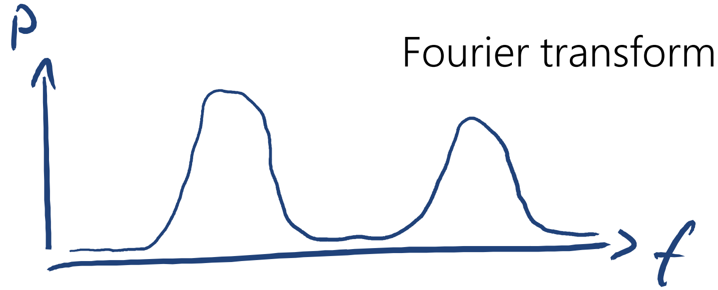

Fourier transform of FID

2D, 3D: Multiple angles & filtered back-projection à la CT

Spatial Encoding and Reconstruction in *k*-Space

- Slice selection
  - Enable longitudinal gradient field G_z during RF pulse
  - Excite only selected slice
- Frequency encoding gradient
  - Enable gradient field G_x perpendicular to G_z after RF pulse
  - Precession frequency varies in *x* direction (e. g. "column")
- Phase encoding gradient
  - For a short period after the RF pulse, enable a gradient field G_y perpendicular to both G_x and G_z
  - Precession phase shift in *y* direction (e. g. "row")
- Signal S generated by precessing spins (Ljunggren 1983, Twieg 1983)
  - $S(k_x, k_y) = \iint_\Omega M_{xy}(x,y)e^{i(k_x x + k_y y)}\,dx\,dy$ — Fourier transform!
  - With $k_x \coloneqq \gamma G_x t$ and $k_y \coloneqq \gamma n \Delta G_y \tau$
- iFFT for reconstruction (or more sophisticated techniques ...)

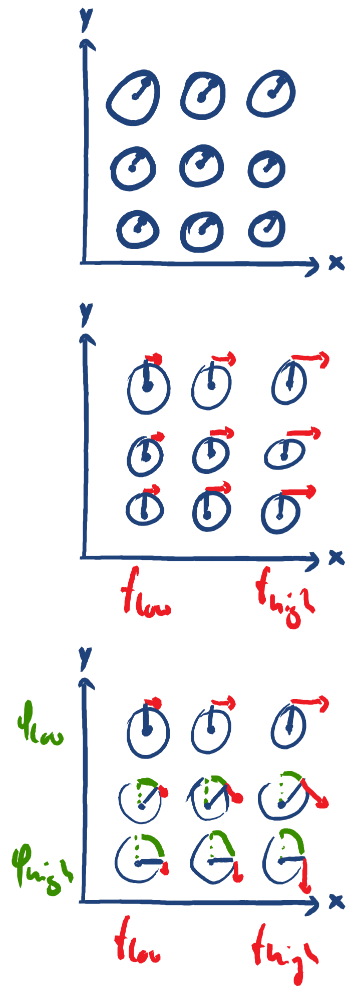

Pros and Cons

- No ionizing radiation, no (known) long-term effects
- Excellent soft-tissue imaging
- Spatial resolution: ~ 1 mm (clinical; micro MRI: < 20 µm)
- Real-time capable (~ 20-30 ms temporal, 1.5-3.0 mm spatial resolution)

- More expensive than CT
- More time consuming than CT
- “Projectile risk”
- RF fields heat tissue & interfere with pace makers, cochlear implants
- Peripheral nerve stimulation (PNS)
- Acoustic noise (up to 120 dB(A))
- “Quenches”
- Claustrophobia, discomfort

Imaging Techniques | Magnetic Resonance Imaging | MRI Safety

http://simplyphysics.com/flying_objects/M

http://simplyphysics.com/flying_objects/FloorPolisher.JPG

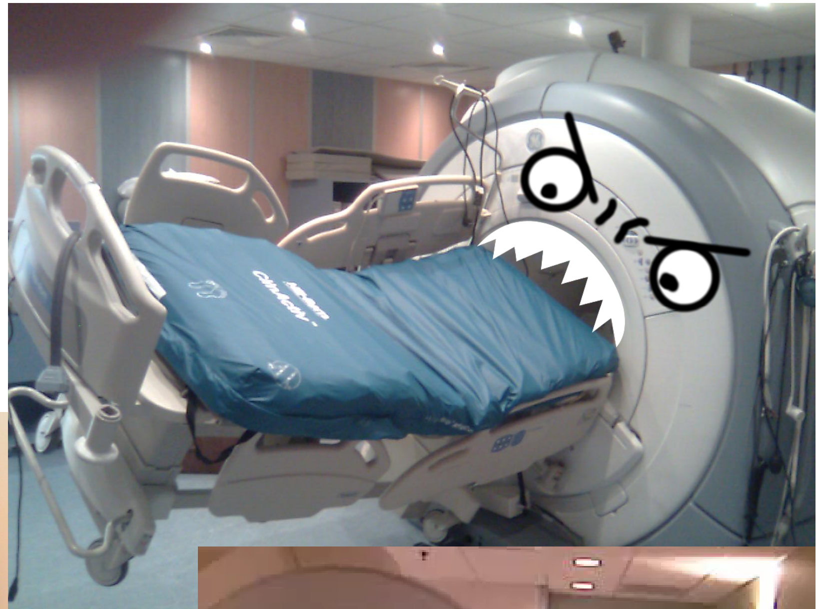

“Quenches”

https://www.youtube.com/watch?v=9SOUJP5dFEg

Clinical MRT

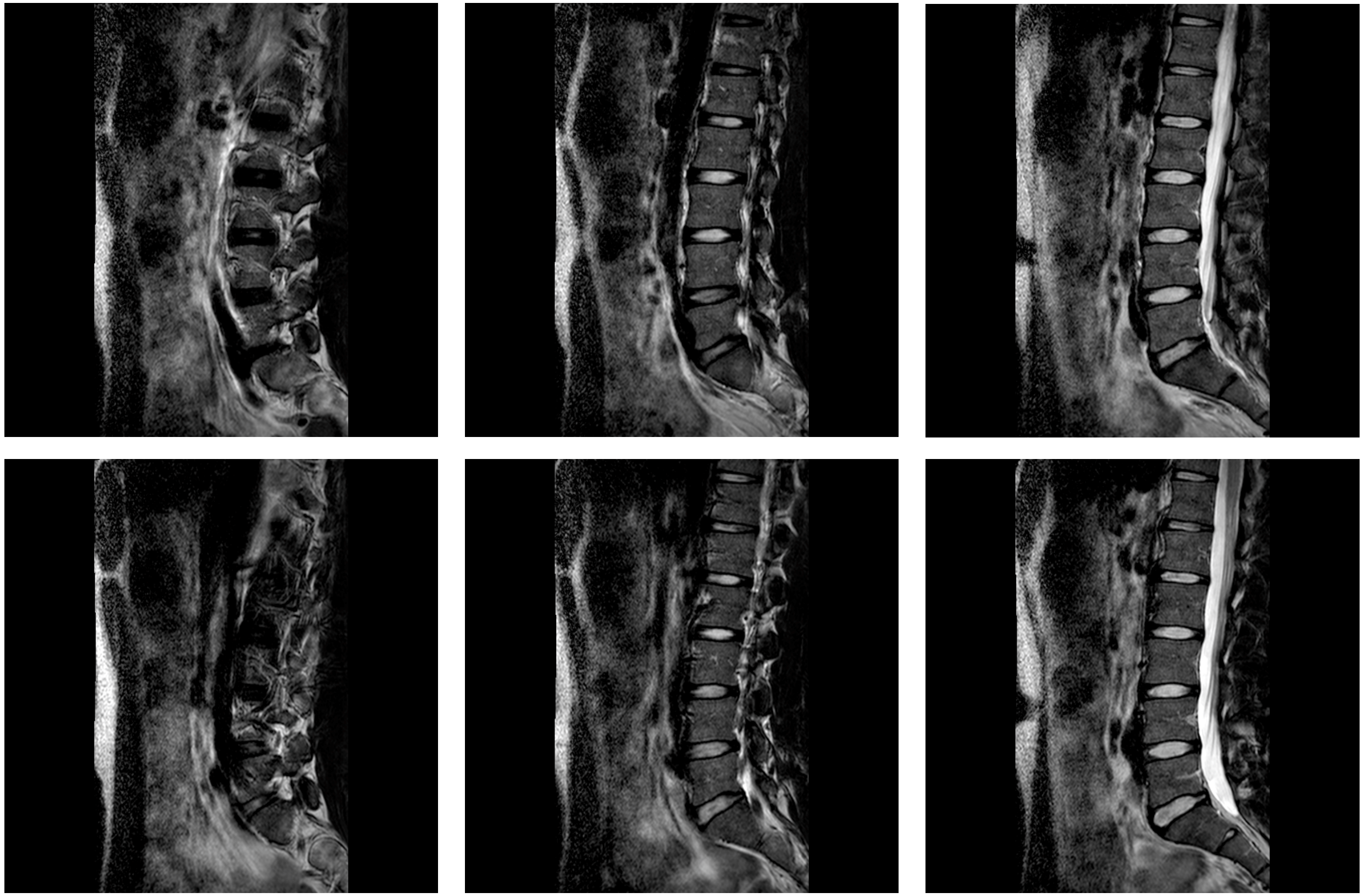

Clinical MRT @ 3 T
T2-weighted
Lumbar spine

Thanks to Niki Berger-Roscher!

Imag

Cli

Clinica
“Speci
Long s
500 μr
Motio

Thank

Micro MRT

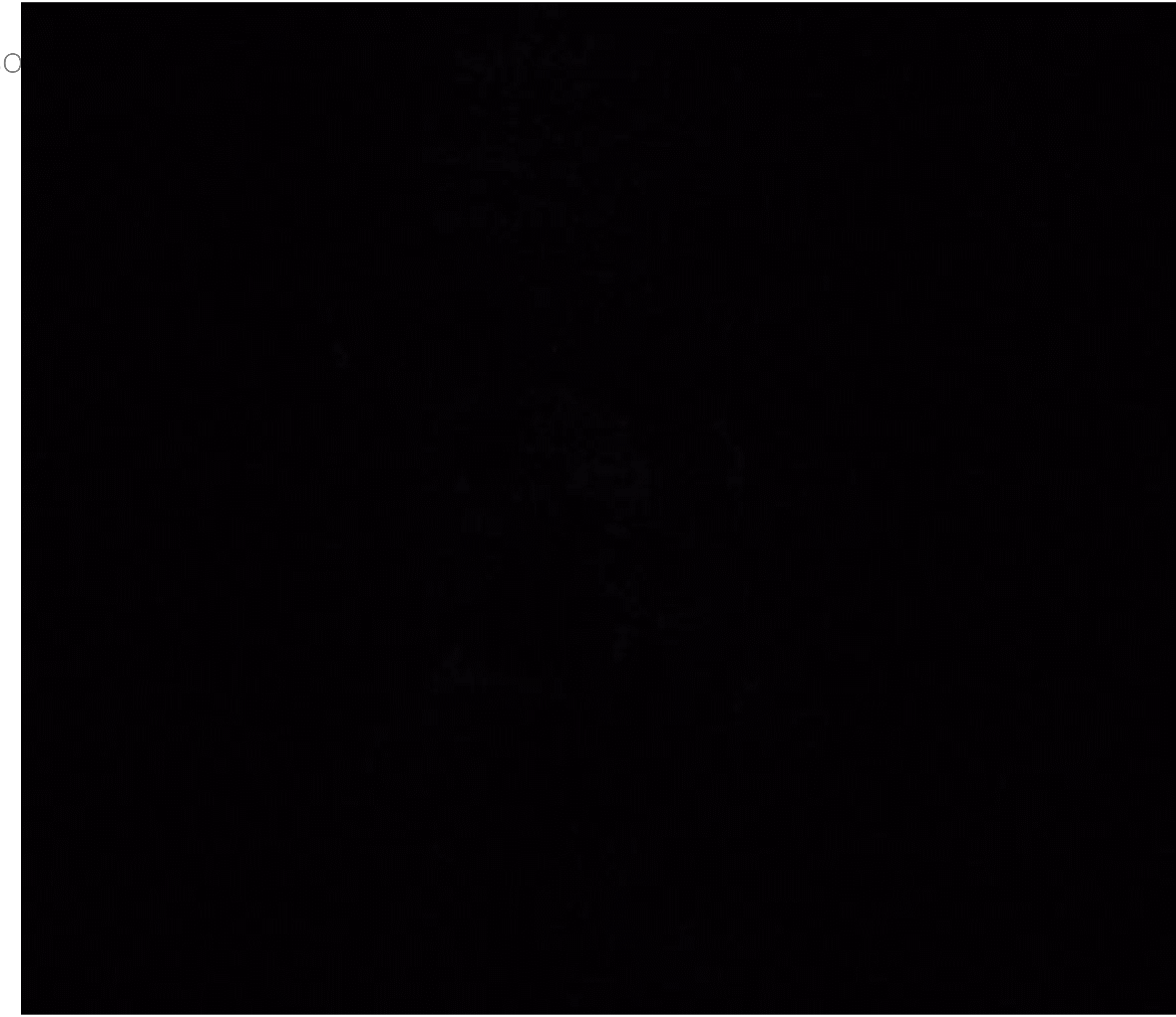

Micro MRT @ 11.7 T
70 µm
Bovine tail

Thanks to Niki Berger-Roscher!

Non-Invasive Anatomical Imaging Techniques

Most widely used for comp. biomech. applications:

(X-ray) computed tomography (CT)

- Ionizing X-ray photons
- Excellent hard-tissue imaging

Magnetic resonance imaging

- Nuclear magnetic resonance, spin echo
- Excellent soft tissue imaging

Ultrasonography

- Ultrasonic/-sound waves (mechanical waves)
- Lower overall image quality, but „hazard-free“, real-time & inexpensive

Ultrasonography

- Basic principle:
  - Emit ultrasound (US) pulse
  - Measure round-trip time(s) and intensity of echo(s)
  - Repeat for each scan-line
  - Reconstruct 2D image (slice) by estimating location/depth of US reflections
- Transducer generates US pulses and picks up echos
  - HF ultrasound (1 … 20 MHz range)
  - Generated by piezo-electric elements
  - Echos create electric field in turn
  - Multiple "scan-lines"
  - 2D-array transducers for 3D real-time imaging

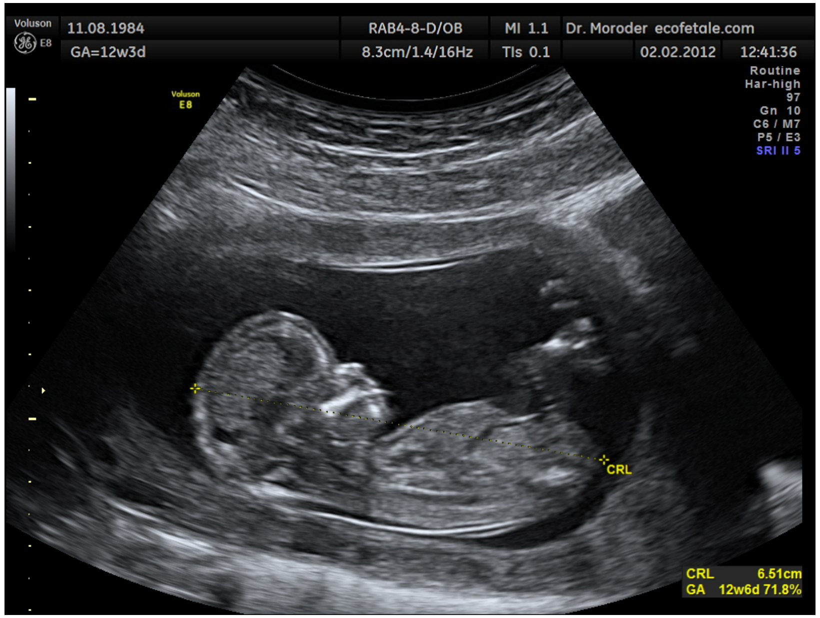

wikimedia.org

(Specular) Reflection on Tissue Boundaries

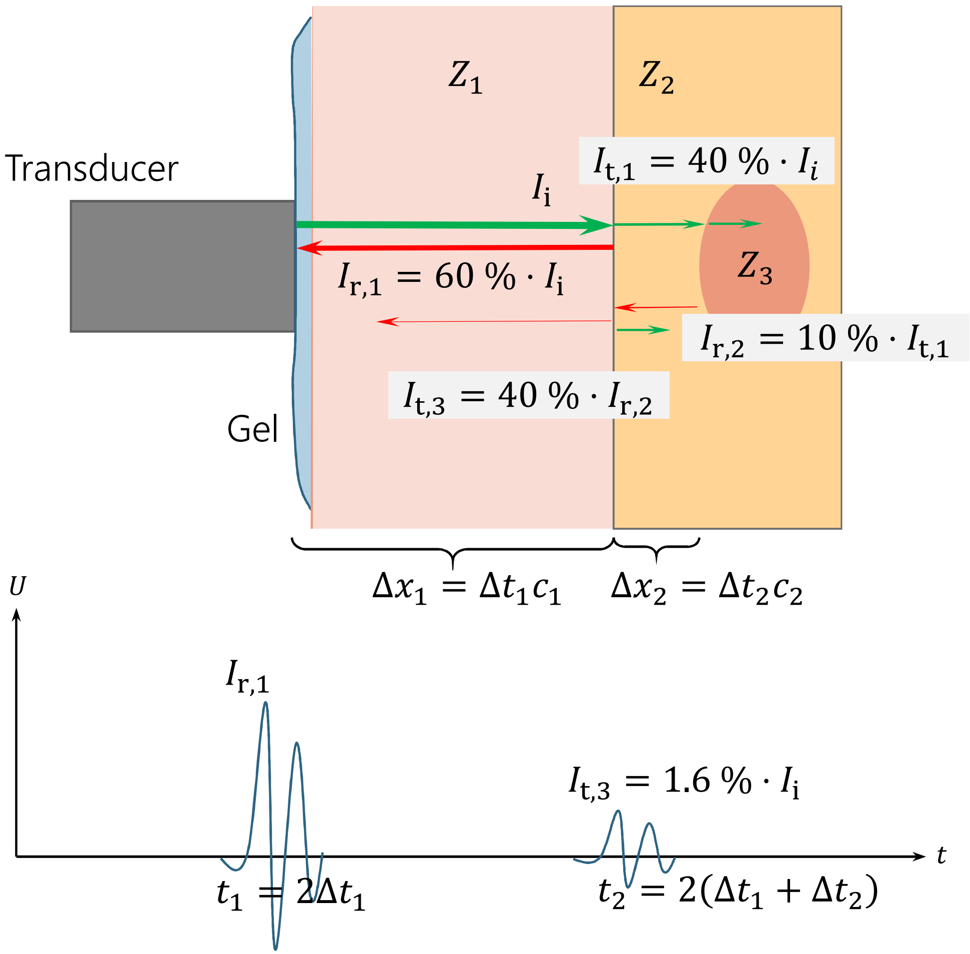

Reflected energy $I_\mathrm{r} = I_\mathrm{i} R \cos\theta$

Reflection coefficient $R = (Z_1 - Z_2)^2/(Z_1 + Z_2)^2$

- Muscle ↔ fat: 6.7 %
- Muscle ↔ bone: 56 %
- Muscle ↔ air: 98 %

Acoustic impedance $Z = \rho c$ in $\mathrm{Pa\,s/m} = \mathrm{rayl}$ (Rayleigh)

- Air: 400 rayl
- Water: $1.5 \cdot 10^6$ rayl
- Muscle: $1.7 \cdot 10^6$ rayl
- Bone: $7.8 \cdot 10^6$ rayl

Transmission coefficient $T = 1 - R = 4Z_1 Z_2/(Z_1 + Z_2)^2$

Scattering (Diffuse Reflection) & Interference

- Reflections on small (~ wave length) “scatterers”, material “impurities”, rough surfaces
- Scatters incident US in all directions (diffuse reflection)
- Interference of scattered US
  - In-phase: constructive
  - Out-of-phase: destructive
- Results in “speckle” noise
  - May provide useful diagnostic information

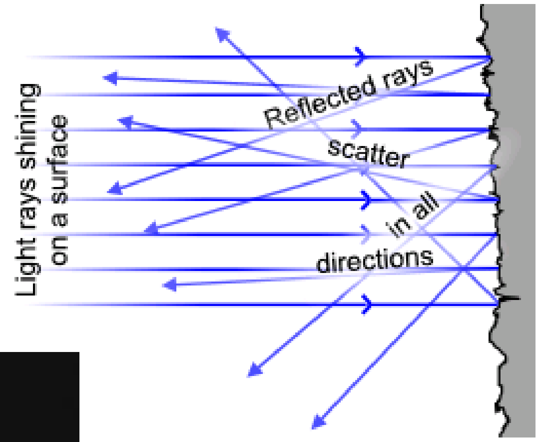

wikimedia.org

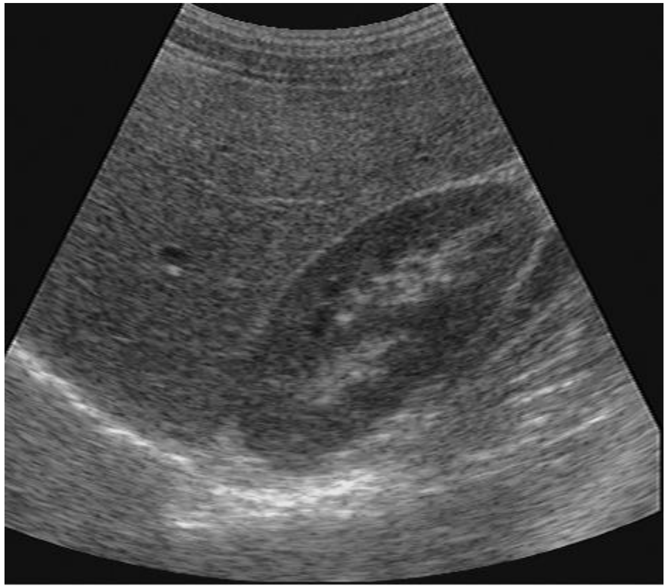

http://mi.eng.cam.ac.uk/~rwp/proj2004/proj4_04.html

Refraction & Diffraction

- Refraction:
  - Direction of propagation changes at interfaces of media with different sound velocities
  - Snell's law $\sin\theta_{\mathrm{i}}/\sin\theta_{\mathrm{t}} = c_1/c_2$
  - Typically rather weak effect in tissues with similar longitudinal sound velocities
- Diffraction:
  - Figuratively: wave "bends around corner"
  - Huygens-Fresnel principle: Every point on the wave front is origin of an "elementary wave"
    - Superposition (& interference) of elementary waves → new wave front
  - Weak for HF sound waves

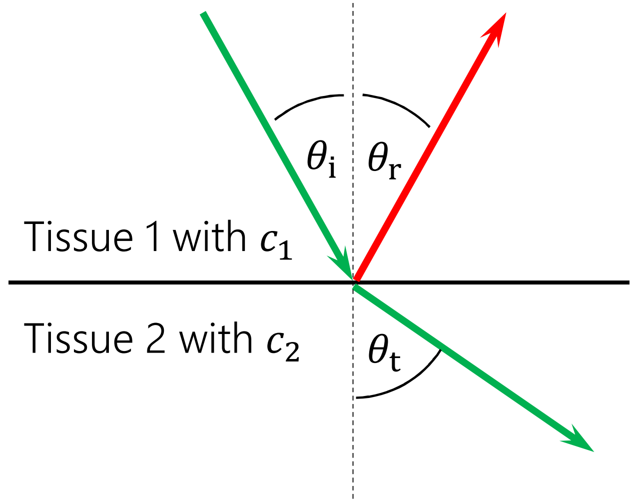

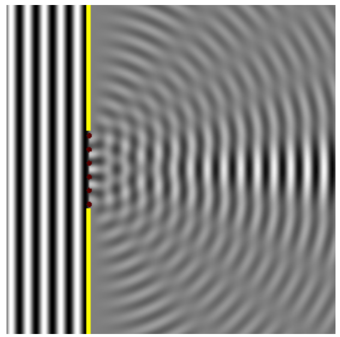

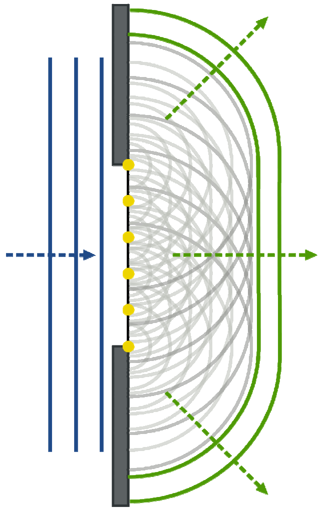

wikimedia.org

Acoustic Attenuation

- Reduction in amplitude with the traveled distance due to
  - Absorption (viscoelasticity!) and
  - Scattering & destructive inference

$$I(s) = I_0 e^{-\alpha f s}$$

α: attenuation coefficient in 1/(cm MHz)

Water: $0.002\ \mathrm{dB/(cm\ MHz)}$
Blood: $0.2\ \mathrm{dB/(cm\ MHz)}$
Muscle: $1.1\ \mathrm{dB/(cm\ MHz)}$
Cortical bone: $6.9\ \mathrm{dB/(cm\ MHz)}$
Trabecular bone: $9.9\ \mathrm{dB/(cm\ MHz)}$
Cranial bone: $15\ \mathrm{dB/(cm\ MHz)}$
Lung: $40\ \mathrm{dB/(cm\ MHz)}$

Conversion from dB/(cm MHz): $\alpha = \frac{\ln(10)}{10}\alpha_{\mathrm{dB}}$

f: frequency of US
s: distance travelled in medium

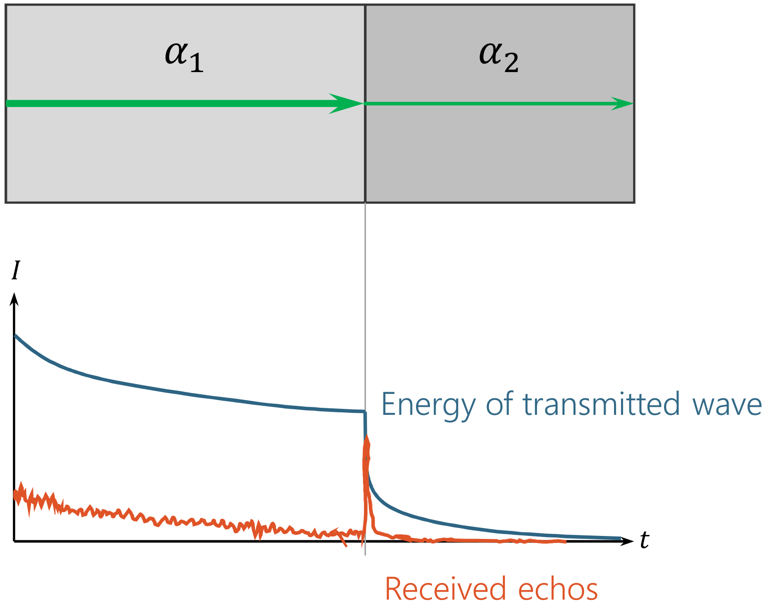

Resolution-Penetration Trade-Offs

- US pulses: multiple of wave length
  $\lambda = c/f = cT$
- Echo separation: $\Delta t > nT$
- Depth resolution: $\Delta x > n\lambda$
- Higher frequency implies …
  - … shorter pulse length → increased resolution
  - … quicker attenuation → decreased penetration depth
- Repetition period limits temporal resolution

$$t_{1,e} = t_{1,s} + nT$$

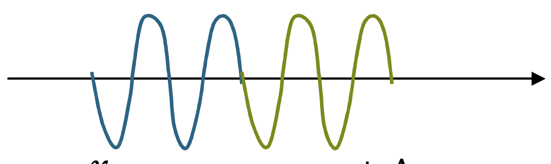

$$t_{1,s} = \frac{x_1}{c} \qquad t_{2,s} = \frac{x_1 + \Delta x}{c}$$

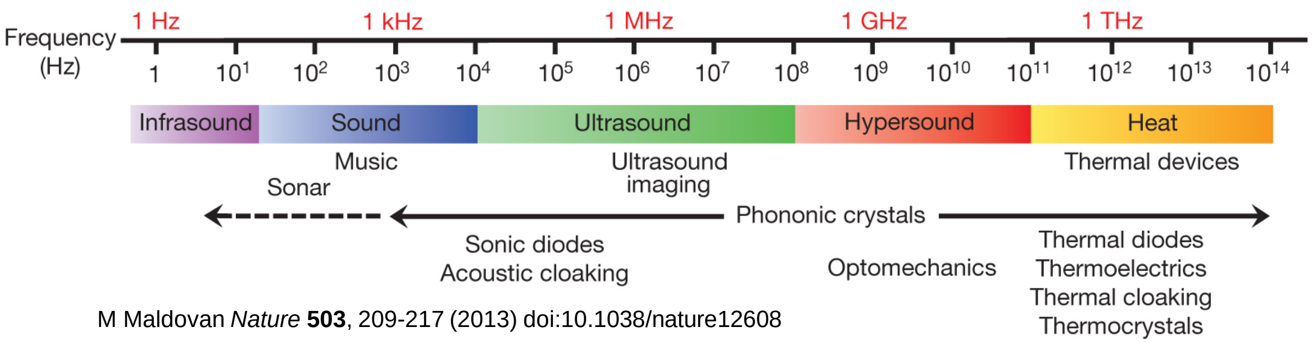

M Maldovan *Nature* **503**, 209-217 (2013) doi:10.1038/nature12608

Post-Processing & Image Reconstruction

- Compensate attenuation (gain)
- Dynamic range compression
- Demodulation (rectification + low-pass filter)
- Image reconstruction (per scan-line)
- Artifacts, e.g.

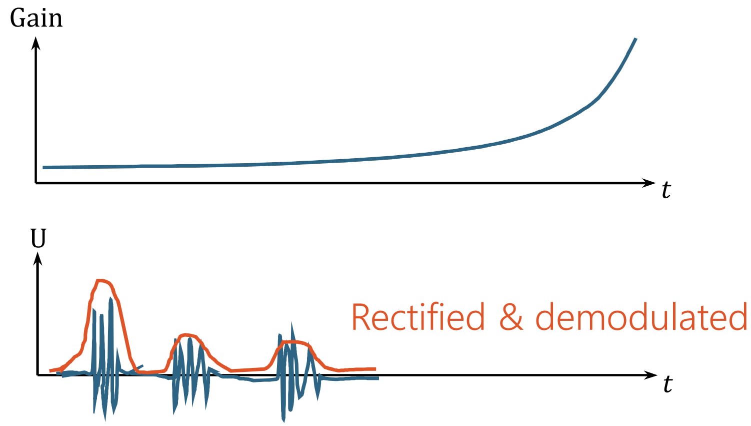

radiopedia.org

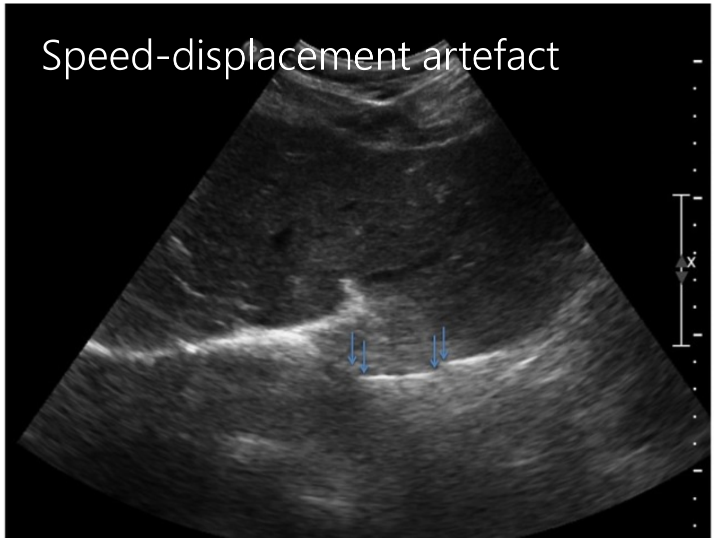

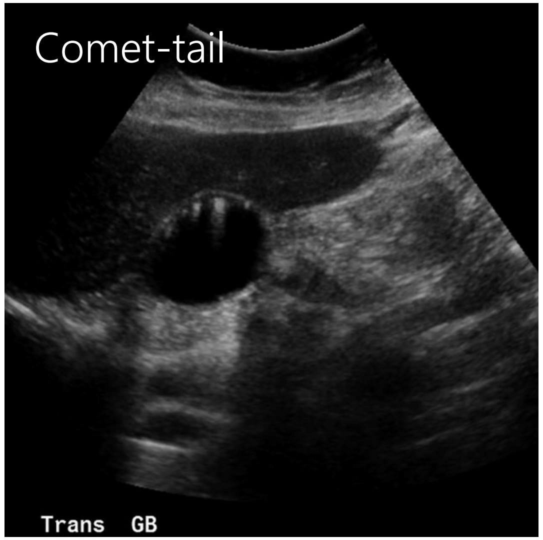

Pros & Cons

- No ionizing radiation, no (known) long-term effects (aside from heating @ high power)
- Real-time capable (up to 1000 fps)
- Inexpensive
- Portable
- Optional 3D imaging
- Direct depth information (no projection)
- Speed measurements (Doppler effect)
- Excellent resolution *possible* (3 – 5 µm resolution @ 15 … 80 MHz)

- Limited penetration depth (in particular at high frequencies)
- Shadowing by bone, gas (almost impenetrable)
- Slices can be hard to interpret
- Good images require high level of skill